# Modelling a Population in a Moving Habitat

Jane Shaw MacDonald

Thesis submitted to the Faculty of Graduate and Postdoctoral Studies in partial fulfillment of the requirements for the degree of
Master of Science in Mathematics[1]

Department of Mathematics and Statistics
Faculty of Science
University of Ottawa



[1]The M.Sc. program is a joint program with Carleton University, administered by the Ottawa-Carleton Institute of Mathematics and Statistics

# Abstract

The earth's climate is increasing in temperature and as a result many species' habitat ranges are shifting. The shift in habitat ranges threatens the local persistence of many species. Mathematical models that capture this phenomena of range shift do so by considering a bounded domain that has a time dependant location on the real line. The analysis on persistence conditions has been considered in both continuous-time and -space, and discrete-time, continuous-space settings. In both model types density was considered to be continuous across the boundaries. However it has been shown that many species exhibit particular behaviour at habitat edges, such as biased movement towards the more suitable habitat. This behaviour should be incorporated into the analysis to obtain more accurate persistence conditions. In this thesis persistence conditions are obtained for generalized boundary conditions with a continuous-time and -space model for a range-shifting habitat. It is shown that a high preference for the suitable habitat at the trailing edge can greatly reduce the size of suitable habitat required for species persistence. As well, for fast shifting ranges, a high preference at the trailing edge is crucial for persistence.

# Dedications

Dedicated with love to my family, whose encouragement to follow my dreams has ever given me the strength to do so.

# Acknowledgement

Acknowledgments go to my supervisor Professor Frithjof Lutscher for his excellent guidance and support throughout this project. As well acknowledgments go to NSERC and the University of Ottawa for their financial support.

# Contents

**List of Figures** **vii**

**1 Introduction** **1**

**2 Literature Review** **3**
2.1 Mathematical Background . . . . . 3
2.2 Introduction to the Critical Patch-Size . . . . . 5
2.3 The Importance of Boundary Conditions . . . . . 7
2.4 Modelling Behaviour at Interfaces . . . . . 8
2.5 Critical Patch-Size with Interface Behaviour . . . . . 11
2.6 A Moving Habitat . . . . . 12
2.7 Two Species In A Moving Habitat . . . . . 16

**3 The Model** **20**
3.1 The Master Equation . . . . . 20
3.2 Transforming to a Fixed Spatial Domain and Nondimensionalization . . . . . 23

**4 Analysis of the Nondimensionalized Equation** **25**
4.1 Linearization and the Eigenvalue Problem . . . . . 25
4.2 Steady States and Their Stability . . . . . 27
4.3 The Critical Patch-Size . . . . . 32
4.3.1 Case 1: A negative radicand . . . . . 33
4.3.2 Case 2: A positive radicand . . . . . 35

**5 Illustrating The Critical Patch-Size** **39**
5.1 Case 1: The Critical Patch-Size for $c < 2$ . . . . . 39
5.1.1 The Critical Patch-Size as a Function of $D_1$ and $D_2$ . . . . . 39
5.1.2 The Critical Patch-Size as a Function of $\alpha$ and $\beta$ . . . . . 41
5.2 Case 2: The Critical Patch-Size for $c \geq 2$ . . . . . 45

**6 Discussion** **49**
6.1 Mathematical Results . . . . . 49
6.2 Future Work . . . . . 50

**A Derivation of the Heat Equation via a Random Walk** **53**

**Bibliography** **55**

**Index** **55**

# List of Figures


2.1 Recreation of Fig. 1 from [3]. . . . . 14
2.2 Recreation of Fig. 2 from [3] . . . . . 15

3.1 Illustration of arrangement of suitable and unsuitable habitat . . . . 21

4.1 Phase portrait for $c < 2$ . . . . . 34
4.2 Phase portrait for $c \geq 2$ with no connection . . . . . 36
4.3 Phase portrait for $c \geq 2$ with connection . . . . . 37

5.1 $L^*_{c<2}$ as a function of the parameter $D_1$ . . . . . 40
5.2 $L^*_{c<2}$ as a function of the parameter $D_2$ . . . . . 41
5.3 $L^*_{c<2}$ as a function of the parameter $\alpha$ when $\beta$ is large . . . . . 42
5.4 $L^*_{c<2}$ as a function of the parameter $\alpha$ when $\beta$ is small . . . . . 43
5.5 A close up of $L^*_{c<2}$ as a function of the parameter $\alpha$ when $\beta$ is large 44
5.6 $\gamma_0^\beta$ as a function of the parameter $c$ . . . . . 44
5.7 $L^*_{c\geq 2}$ as a function of the parameter $\alpha$ when $\beta$ is large . . . . . 46
5.8 $L^*_{c\geq 2}$ as a function of the parameter $\alpha$ when $\beta$ is small . . . . . 47
5.9 A close up of $L^*_{c\geq 2}$ as a function of the parameter $\alpha$ when $\beta$ is large 48

# Chapter 1

# Introduction

How much suitable habitat does a species need in order to persist? This question is at the heart of conservation ecology. In general, the ability of a species to persist in a suitable, stationary habitat does not only depend on fecundity but also on the size of the given habitat. This is because individuals disperse and thereby may leave the suitable habitat. The balance of gain from fecundity and loss from dispersal can be characterized by the size of the habitat. When the habitat is large enough, individuals stay in the habitat longer for the simple reason it takes more time for them to reach the boundary. Accordingly, there is a critical habitat size above which a population can persist [12, 6, 8].

The earth's climate is changing. Average global temperatures have been increasing for the last century and are expected to continue to rise at an even faster rate [1]. As a result, the suitable habitats for many species are shifting either poleward in latitude or upwards in elevation [14]. For many species, this shift presents a real threat to their local existence. When the suitable habitat is stationary, individuals who are almost stationary are very likely to remain in the habitat. However, if the ranges are shifting, then individuals who move very little will find themselves outside of the suitable habitat much more quickly. Thus, the size of the habitat needed to sustain a population may be different depending on whether and how fast the habitat moves. These ecological observations give rise to the question: "Can a species persist in a moving habitat?"

This question has been addressed via mathematical modelling in several recent publications, starting with the work of Potapov and Lewis [10] and Berestycki et al. [3] and recently applied to butterfly data by Leroux et al. [7]. All these models are based on reaction-diffusion equations, continuous in space and time, that assume that population growth and dispersal occur on the same time scale. Corresponding results in discrete-time models were analyzed by Harsch et al. [5] and Zhou and Kot [15].

All these approaches model the suitable habitat as a bounded interval on the real

line and include the effects of climate change by making the location of the habitat time dependent. All approaches define population persistence as the linear instability of the trivial (zero) steady state. All models come to the conclusion that when the habitat moves faster, it needs to be longer to sustain the population. And all models find a threshold speed of the habitat above which the population will go extinct no matter how long the habitat is.

None of the models mentioned above, however, contain a detailed description of the movement behaviour at the interfaces between the suitable habitat and its unsuitable surroundings. Empirical research has shown that many species exhibit specific behaviour at the edges of their habitats such as movement bias towards the suitable habitat. This aspect was only recently included into reaction-diffusion models with fixed suitable habitats by Maciel and Lutscher [9]. They showed that the correct inclusion of this boundary behaviour is crucial for a correct prediction of the fate of the population. Mathematically, the new model indicates that the population density across an interface may be discontinuous, whereas all previous models assumed continuity. In particular, climate change models have not included this movement behaviour into the analysis.

In this thesis, I ask the question: "How does edge behaviour of individuals affect the ability of a population to persist on a moving habitat?" In the next chapter, I give a review of the current literature relevant to my thesis. In the subsequent chapters, I present my model and generalize the work in [10] and [3] by adding the interface conditions suggested in [9]. I illustrate my results and close with a discussion of the differences, mathematical and ecological, between my results and the previous ones. From this analysis I find that, when including edge behaviour of individuals on a moving habitat, conditions on population persistence surprisingly vary from the current literature.

# Chapter 2

# Literature Review

In this chapter, I start by presenting some theory around reaction-diffusion equations (RDEs), following Chapter 2 of [4]. I introduce a general model, continuous in both space and time, that has been suggested to describe population densities in spatial ecology. I present certain properties of the eigenvalue problem corresponding to the linearized model.

I then give a detailed account of the history of the critical patch-size as an integral element in the studies of mathematical spatial ecology. I will introduce this concept by following Skellam [12], who considers a simple reaction-diffusion equation coupled with linear growth on a bounded domain. The author derives a critical patch-size from the condition that the zero state of the model be unstable. I discuss the importance of boundary conditions for the critical patch-size.

Next, I review the work of Maciel and Lutscher [9], who use a random walk to derive matching conditions for population density and flux at an interface between two adjacent habitat types. From these interface conditions, one can derive generalized boundary conditions. The critical patch-size is then derived for a model with these generalized boundary conditions.

Finally, I present the models and some relevant results from two papers that deal with the question of a critical patch-size in a climate-change scenario. In this case, the patch is not stationary in time but moves in space at a constant speed. The paper by Berestycki et al. [3] looks at the problem for a single species from a geometrical point of view with phase-plane analysis. The paper by Potapov and Lewis [10] considers two competing species and derives a related eigenvalue problem to determine the critical patch-size.

## 2.1 Mathematical Background

To apply reaction-diffusion equations in spatial ecology, one denotes the density of a population in space $x$ and time $t$ as $u(x,t)$. In the simplest case, one assumes that

individuals move randomly in space and arrives at the well-known diffusion equation

$$u_t = Du_{xx}, \tag{2.1.1}$$

where subscripts denote partial derivatives. This equation can be derived in several ways. A derivation from an unbiased random walk is given in Appendix A.

To model how individuals reproduce and die, one writes the ordinary differential equation $u'(t) = f(u)$, where a famous example is the logistic growth function $f = ru(1 - u/K)$. Assuming that movement and population dynamics occur on the same timescale, one combines the dynamics with (2.1.1) and obtains the reaction-diffusion equation

$$u_t = Du_{xx} + f(u). \tag{2.1.2}$$

If the growth function depends on the spatial location, one writes $f(u, x)$. For example, the parameters $r$ and $K$ of the logistic equation might depend on space.

If the population resides in a bounded domain, say some interval $[0, L]$, one needs to impose conditions at the boundary to make the problem well-posed. The two standard boundary conditions are the Dirichlet (or hostile) conditions

$$u(t, 0) = u(t, L) = 0, \tag{2.1.3}$$

and the Neumann (or no flux) conditions

$$u_x(t, 0) = u_x(t, L) = 0. \tag{2.1.4}$$

The former corresponds to individuals who reach the boundary leaving the domain with probability one; the latter corresponds to individuals staying in the domain with probability one. Intermediate cases are modelled by so-called Robin conditions

$$u_x(t, 0) = \gamma(0)u(t, 0), \qquad u_x(t, L) = \gamma(L)u(t, L), \tag{2.1.5}$$

with $\gamma(0) \geq 0$ and $\gamma(L) \leq 0$.

In ecological applications, it is typical to have $f(0) = 0$, which means that individuals cannot appear out of nothing. Therefore, the reaction-diffusion equation has $u^*(x) = 0$ as a steady state solution, corresponding to the absence of the population. One is interested in whether there are positive steady state solutions, corresponding to the existence of a population. It turns out that, in some cases, the existence of a positive steady state solution is closely related to the stability of the zero solution. This problem can be formulated more generally as follows.

Consider the reaction-diffusion equation

$$u_t = (d(x)u_x)_x + f(x, u), \qquad x \in (0, L), \tag{2.1.6}$$

with boundary conditions

$$d(x)u_x = \gamma(x)u, \qquad x = 0, L, \quad t > 0. \tag{2.1.7}$$

The corresponding eigenvalue problem is given by

$$\lambda\phi(x) = (d(x)\phi_x)_x + r(x)\phi, \qquad x \in (0, L), \tag{2.1.8}$$

where $r(x) = f_u(x, 0)$, with boundary conditions as in (2.1.7).

The following result can be found as Proposition 3.2 in [4].

**Proposition 2.1.** *Assume that the growth function can be written as $f(x, u) = g(x, u)u$ where $g$ is a smooth function, decreasing in $u$, and there exists a positive constant $K$ such that $g(x, u) < 0$ for $u > K$. If the largest eigenvalue of (2.1.8), with boundary conditions corresponding to (2.1.7), is positive, then there exists a minimal positive steady state solution $u^*(x)$ of (2.1.6) – (2.1.7). Furthermore, all solutions of the nonlinear problem whose initial conditions are non-negative in $(0, L)$ and positive on a subinterval are eventually bounded below by orbits that increase towards $u^*$ as $t \to \infty$.*

For this reason, it is important to study the linear stability of the zero solution. Eigenvalue equations of the form in (2.1.8), with corresponding boundary conditions of the form (2.1.7), are well studied as so-called Sturm–Liouville problems. Their first important property is that there are countably many, real, ordered eigenvalues. Secondly there exists one eigenvalue larger then all the others, called the dominant eigenvalue, that is

$$\lambda_1 > \lambda_2 \geq ...\lambda_k \geq ... \qquad \text{with} \qquad \lambda_k \to -\infty \tag{2.1.9}$$

as $k \to \infty$. The third important property is that the eigenfunction corresponding to the dominant eigenvalue is of one sign in $(0, L)$ and hence can be chosen to be positive.

The last statement relevant to my thesis is about the dominant eigenvalues' continuous dependence on model parameters. It is presented as Corollary 2.2 following Theorem 2.1 in [4] and is summarized as the following result.

**Proposition 2.2.** *Suppose that $d(x) \geq d_0 > 0$ and that $\gamma(0)$ is positive and $\gamma(L)$ is negative. Denote $\lambda$ to be the dominant eigenvalue of system (2.1.8) with boundary conditions corresponding to (2.1.7). Then $\lambda$ is a decreasing function with respect to $|\gamma|$ in the sense that if $|\gamma_1(x)| > |\gamma_2(x)|$, then $\lambda(|\gamma_1(x)|) < \lambda(|\gamma_2(x)|)$.*

This result will be used in Chapter 4 in a proof on stability of the steady states for my model.

## 2.2 Introduction to the Critical Patch-Size

The concept of the critical patch-size was first introduced by Skellam in 1951 [12] and independently by Kierstead and Slobodkin in 1953 [6]. They used the linear

reaction-diffusion equation with Dirichlet boundary conditions; i.e., their model was

$$u_t = Du_{xx} + ru, \qquad 0 < x < L, \quad t > 0, \tag{2.2.1}$$
$$u(0,t) = 0 = u(L,t), \qquad t > 0. \tag{2.2.2}$$

The Dirichlet conditions serve as a 'worst case' in terms of persistence. If a population can persist when all individuals at the boundary leave the domain, then it can certainly persist if not all individuals leave the domain; i.e., when we have some mixed boundary (Robin) conditions.

Plugging the ansatz $u(x,t) = X(x)T(t)$ into equation (2.2.1) implies that $T$ and $X$ solve the following differential equations,

$$T'(t) = \lambda T(t), \tag{2.2.3}$$
$$DX''(x) + rX(x) = \lambda X(x), \tag{2.2.4}$$

where $\lambda$ is an eigenvalue for the system. It will eventually be determined by the boundary conditions. In general, solutions to this system are

$$T(t) = Ae^{\lambda t}, \tag{2.2.5}$$
$$X(x) = Be^{nx} + Ce^{-nx}, \tag{2.2.6}$$

where $n = \sqrt{\frac{\lambda - r}{D}}$. In particular, solutions are subject to the boundary conditions $X(0) = 0 = X(L)$. Nontrivial solutions that satisfy these boundary conditions exist only when $\lambda - r < 0$. Thus, solutions may be written as a linear combination of sine and cosine

$$X(x) = B\cos\left(\sqrt{\frac{r-\lambda}{D}}x\right) + C\sin\left(\sqrt{\frac{r-\lambda}{D}}x\right). \tag{2.2.7}$$

Application of the boundary condition at $x = 0$ gives $B = 0$. Application of the boundary condition at $x = L$ results in the condition

$$\sqrt{\frac{r-\lambda}{D}}L = m\pi, \qquad m \in \mathbb{N}, \tag{2.2.8}$$

implying that the eigenvalues are given by

$$\lambda = \lambda_m = r - D\left(\frac{m\pi}{L}\right)^2. \tag{2.2.9}$$

Thus, the solution of the problem on the bounded domain is

$$u(x,t) = \sum_{m=1}^{\infty} A_m e^{\lambda_m t}\sin\left(\frac{m\pi}{L}x\right), \tag{2.2.10}$$

where $A_m$ are the Fourier coefficients given by the initial condition.

If $\lambda_m < 0$ for all $m$, then all solutions decay to zero over time. If $\lambda_m > 0$ for at least one $m$, then there is a solution that does not decay to zero. Since $\lambda_m$ is a decreasing function of $m$, the stability of $u = 0$ is decided by the sign of $\lambda_1$. If $\lambda_1 > 0$, the zero solution is unstable; if $\lambda_1 < 0$, it is stable. The critical value is $\lambda_1 = 0$.

As $\lambda_1$ is a function of the parameter $L$, the stability of the steady state can be characterized by the length of the domain. Thus, the bifurcation point $\lambda_1 = 0$ for the zero equilibrium is given in terms of the domain length as

$$L^* = \pi\sqrt{\frac{D}{r}}. \tag{2.2.11}$$

For $L > L^*$ we have $\lambda_1 > 0$ and the population can persist. For $L < L^*$, the population goes extinct. The bifurcation point $L^*$ has since been termed the 'critical patch-size'.

## 2.3 The Importance of Boundary Conditions

In the previous section, Dirichlet conditions were imposed at the boundary for system (2.2.1). In the case where Neumann conditions are imposed, the issue of a critical patch-size does not arise. Indeed, consider again system (2.2.1), but now impose the boundary conditions

$$u_x(0,t) = 0 = u_x(L,t), \qquad t > 0. \tag{2.3.1}$$

As in the previous section, solutions are found by the method of seperation of variables assuming $u(x,t) = X(x)T(t)$. This gives the solutions (2.2.5) and (2.2.6) and the boundary conditions $X'(0) = 0 = X'(L)$. The right-hand boundary condition implies that $B = C$. The left-hand boundary condition implies that

$$e^{2\sqrt{\frac{\lambda-r}{D}}L} = 1. \tag{2.3.2}$$

For $\lambda = r$, the solution for $X$ is a constant. All other solutions are found by assuming $\lambda - r < 0$, and thus solutions may again be written as in (2.2.7). The right-hand boundary condition gives $C = 0$. The left-hand boundary condition results in condition (2.2.8), thus again implying

$$\lambda = \lambda_m = r - D\left(\frac{m\pi}{L}\right)^2, \qquad m \in \mathbb{N}. \tag{2.3.3}$$

Thus solutions to the problem with Neumann boundary conditions and some initial condition $u(x,0) = g(x) > 0$ is

$$u(x,t) = \sum_{m=0}^{\infty} A_m e^{\lambda_m t}\cos\left(\frac{m\pi}{L}x\right), \tag{2.3.4}$$

where the coefficients $A_m$ can be obtained from the initial condition. Here the dominant eigenvalue is $\lambda = r$, and, since $r > 0$, the dominant eigenvalue is always positive. Thus, a nonnegative solution exists independent of model parameters, particularly independent of $L$. Hence the critical patch-size could be said to be $L^* = 0$.

This suggests that movement behaviour at a boundary plays a crucial role in the analysis of critical patch-size. The next section looks at a random-walk model for movement behaviour at the boundary, where flux and density matching conditions are derived.

## 2.4 Modelling Behaviour at Interfaces

Historically, models considered only the conditions on a favourable patch but not outside. More realistic situations should take into account conditions outside the patch and incorporate individuals' preferences for one or the other type of environment. This is the approach taken by Maciel and Lutscher [9], which I review in this section.

Maciel and Lutscher considered two types of patches, represented by half-lines, that meet at the interface point $x = x_0 = 0$. The half-line to the right (left) of $x_0$ is labelled Patch 1 (Patch 2). Inside patch $i$, individuals perform an unbiased random walk and may take steps of size $\delta_i$, with $p_i$ denoting the probability of moving per time step.

At an interface, an individual moves to patch $i$ with probability $\alpha_i$ and remains at the interface with probability $1 - \alpha_1 - \alpha_2$. To write the master equation, one denotes by $P(l\delta_i, t)\delta_i$ the probability of finding an individual in an interval of length $\delta_i$ around location $l\delta_i$ at time $t$. The master system for the points near the interface then becomes

$$\delta_2 P(-\delta_2, t+\tau) = \frac{p_2}{2}\delta_2 P(-2\delta_2, t) + (1-p_2)\delta_2 P(-\delta_2, t) + \alpha_2\delta_0 P(0,t), \tag{2.4.1}$$

$$\delta_0 P(0, t+\tau) = \frac{p_2}{2}\delta_2 P(-\delta_2, t) + \frac{p_1}{2}\delta_1 P(\delta_1, t) + (1-\alpha_1-\alpha_2)\delta_0 P(0,t), \tag{2.4.2}$$

$$\delta_1 P(\delta_1, t+\tau) = \frac{p_1}{2}\delta_1 P(2\delta_1, t) + (1-p_1)\delta_1 P(\delta_1, t) + \alpha_1\delta_0 P(0,t). \tag{2.4.3}$$

The first step to obtaining the interface conditions is to expand in a Taylor series about $t$ for the terms on the left-hand side and about $-\delta_2$ and $\delta_1$ for the terms including $\pm 2\delta_i$. These Taylor expansions result in the equations

$$\begin{aligned}\delta_2 P(-\delta_2, t) = {} & \frac{p_2}{2}\delta_2 P(-\delta_2, t) + (1-p_2)\delta_2 P(-\delta_2, t) + \alpha_2\delta_0 P(0,t) \\ & + \mathcal{O}(\delta_2\tau) + \mathcal{O}(\delta_2^2),\end{aligned} \tag{2.4.4}$$

$$\begin{aligned}\delta_0 P(0, t) = {} & \frac{p_2}{2}\delta_2 P(-\delta_2, t) + \frac{p_1}{2}\delta_1 P(\delta_1, t) + (1-\alpha_1-\alpha_2)\delta_0 P(0,t) \\ & + \mathcal{O}(\delta_0\tau),\end{aligned} \tag{2.4.5}$$

$$\delta_1 P(\delta_1,t) = \frac{p_1}{2}\delta_1 P(\delta_1,t) + (1-p_1)\delta_1 P(\delta_1,t) + \alpha_1\delta_0 P(0,t) + \mathcal{O}(\delta_1\tau) + \mathcal{O}(\delta_1^2). \tag{2.4.6}$$

Subtracting (2.4.4) multiplied by $\alpha_1$ from (2.4.6) multiplied by $\alpha_2$ and rearranging gives the equation

$$p_2\alpha_1\delta_2 P(-\delta_2,t) = p_1\alpha_2\delta_1 P(\delta_1,t) + \mathcal{O}(\delta_2\tau) + \mathcal{O}(\delta_2^2) + \mathcal{O}(\delta_1\tau) + \mathcal{O}(\delta_1^2). \tag{2.4.7}$$

Equation (2.4.7) divided by $\delta_1$ in the parabolic limit (see Appendix A) as $\delta_1$, $\delta_2$ and $\tau \to 0$ is

$$p_2\alpha_1 \lim_{\delta_1,\delta_2\to 0} \frac{\delta_2}{\delta_1} P(0^-,t) = p_1\alpha_2 P(0^+,t), \tag{2.4.8}$$

where $0^\pm$ denote the limits as $x$ approaches 0 from the right or the left.

The diffusion coefficient, $D$, for a reaction-diffusion equation obtained through a random walk is defined by $D := \lim_{\delta,\tau\to 0} \frac{p\delta^2}{\tau}$; see Appendix A. From equation (2.4.8), it is possible to derive two different conditions for the density across the interface. Both are of the form $P(0^+,t) = kP(0^-,t)$, where $k$ is a measure of the jump in density across the interface. The difference is only in the value of $k$. The first condition is found by assuming $\delta_1 = \delta_2$; i.e., an individual's step size remains the same, independent of the patch. Under this assumption, the multiplication of (2.4.8) by $\frac{\delta_1^2}{\tau}$ in the limit results in

$$k = \frac{\alpha_1}{\alpha_2}\frac{D_2}{D_1}. \tag{2.4.9}$$

The second condition is found by assuming $p_1 = p_2$; i.e., the probability of an individual moving left or right inside a given patch is independent of the patch. Under this assumption, the following holds:

$$\sqrt{\frac{D_1}{D_2}} = \lim_{\delta_1,\delta_2,\tau\to 0} \sqrt{\frac{p_1\frac{\delta_1^2}{\tau}}{p_2\frac{\delta_2^2}{\tau}}} = \lim_{\delta_1,\delta_2\to 0} \frac{\delta_1}{\delta_2}. \tag{2.4.10}$$

In this case, directly taking the limit in (2.4.8) results in

$$k = \frac{\alpha_1}{\alpha_2}\sqrt{\frac{D_2}{D_1}}. \tag{2.4.11}$$

The differences between the two jump measures is not the central analysis of my thesis. For this reason, I continue the analysis with the jump measure as in equation (2.4.11). The differences between the two measures is brought up again in the discussion in Chapter 6.

Matching conditions for the flux at an interface are derived by writing out the following relationship between fluxes at neighbouring locations of the interface

$$D_1\frac{\partial P(0^+,t)}{\partial x}-D_2\frac{\partial P(0^-,t)}{\partial x}=\lim_{\delta_1,\delta_2,\tau\to 0}\left[\frac{\delta_1^2 p_1}{\tau}\frac{P(2\delta_1,t)-P(\delta_1,t)}{\delta_1}+\frac{\delta_2^2 p_2}{\tau}\frac{P(-2\delta_2,t)-P(-\delta_2,t)}{\delta_2}\right]. \tag{2.4.12}$$

The difference $P(2\delta_1,t)-P(\delta_1,t)$ may be rewritten in the following way:

$$\begin{aligned}
P(2\delta_1,t)-P(\delta_1,t) &= \frac{2}{p_1}P(\delta_1,t+\tau)+(p_1-1)\frac{2}{p_1}P(\delta_1,t)\\
&\quad -\alpha_1\frac{\delta_0}{\delta_1}\frac{2}{p_1}P(0,t)-P(\delta_1,t) \qquad \text{(substitute for } P(2\delta_1,t))\\
&= \frac{2}{p_1}P(\delta_1,t)+(p_1-1)\frac{2}{p_1}P(\delta_1,t)\\
&\quad -\alpha_1\frac{\delta_0}{\delta_1}\frac{2}{p_1}P(0,t)-P(\delta_1,t)+\mathcal{O}(\tau)\\
&\qquad\qquad \text{(Taylor expansion about } t)\\
&= P(\delta_1,t)-\alpha_1\frac{\delta_0}{\delta_1}\frac{2}{p_1}P(0,t). \qquad (\tau\to 0)
\end{aligned}$$

Similarly, for the difference $P(-2\delta_2,t)-P(-\delta_2,t)$, I obtain

$$P(-2\delta_2,t)-P(-\delta_2,t)=P(-\delta_2,t)-\alpha_2\frac{\delta_0}{\delta_2}\frac{2}{p_2}P(0,t).$$

Plugging these two relationships into (2.4.12) gives the following computation:

$$\begin{aligned}
&D_1\frac{\partial P(0^+,t)}{\partial x}-D_2\frac{\partial P(0^-,t)}{\partial x}\\
&=\lim_{\delta_1,\delta_2,\delta_0,\tau\to 0}\left[\frac{\delta_1^2 p_1}{\tau}\frac{P(\delta_1,t)_1-\alpha_1\frac{\delta_0}{\delta_1}\frac{2}{p_1}P(0,t)}{\delta_1}+\frac{\delta_2^2 p_2}{\tau}\frac{P(-\delta_2,t)-\alpha_2\frac{\delta_0}{\delta_2}\frac{2}{p_2}P(0,t)}{\delta_2}\right]\\
&=\lim_{\delta_1,\delta_2,\delta_0,\tau\to 0}\left[\frac{\delta_1^2 p_1}{\delta_1\tau}P(\delta_1,t)+\frac{\delta_2^2 p_2}{\delta_2\tau}P(-\delta_2,t)-2\delta_0\left(\frac{\alpha_1}{\delta_1^2 p_1}\frac{\delta_1^2 p_1}{\tau}+\frac{\alpha_2}{\delta_2^2 p_2}\frac{\delta_2^2 p_2}{\tau}\right)P(0,t)\right]\\
&=\lim_{\delta_1,\delta_2,\delta_0,\tau\to 0}\left[\frac{\delta_1 p_1}{\tau}P(\delta_1,t)+\frac{\delta_2 p_2}{\tau}P(-\delta_2,t)-\frac{2\delta_0}{\tau}(\alpha_1+\alpha_2)P(0,t)\right].
\end{aligned}$$

From (2.4.2), I have the relation

$$2\delta_0(P(0,t+\tau)-P(0,t))=p_1\delta_1 P(\delta_1,t)+p_2\delta_2 P(-\delta_2,t)-2(\alpha_1+\alpha_2)\delta_0 P(0,t).$$

Thus,

$$D_1\frac{\partial P(0^+,t)}{\partial x}-D_2\frac{\partial P(0^-,t)}{\partial x}=\lim_{\delta_0,\tau\to 0}\frac{1}{\tau}\big[2\delta_0(P(0,t+\tau)-P(0,t))\big]$$

$$= \lim_{\delta_0,\tau\to 0} \frac{2\delta_0}{\tau}\mathcal{O}(\tau)$$
$$= 0.$$

Consequently, one obtains the conservation of flux across an interface. These matching conditions for flux are found by assuming that the interface is stationary. In my thesis, I will use an adaptation for moving interfaces.

## 2.5 Critical Patch-Size with Interface Behaviour

Maciel and Lutscher [9] applied their interface conditions to a classical model by Ludwig et al. [8]. There is a suitable bounded patch from $x = 0$ to $x = L$ on which the population density follows a reaction-diffusion equation with logistic growth. Outside this patch are two unsuitable patches where individuals die at a constant rate $m > 0$. Hence, the equations are

$$u_t = D_1 u_{xx} + ru(1-u), \qquad \text{for } x \in (0, L), \tag{2.5.1}$$
$$u_t = D_2 u_{xx} - mu, \qquad \text{for } x \notin (0, L). \tag{2.5.2}$$

At the interfaces, the authors imposed matching conditions for density and flux as

$$u(0^+, t) = ku(0^-, t), \tag{2.5.3}$$
$$u(L^-, t) = ku(L^+, t), \tag{2.5.4}$$
$$D_1 u_x(0^+, t) = D_2 u_x(0^-, t), \tag{2.5.5}$$
$$D_1 u_x(L^-, t) = D_2 u(L^+, t). \tag{2.5.6}$$

Ludwig et al. [8] used continuous density matching; i.e., $k = 1$. Maciel and Lutscher [9] use $k$ as in (2.4.9) and (2.4.11) and compared the results. All parameters are assumed positive.

Linearizing the equation in $(0, L)$ at low density gives

$$u_t = D_1 u_{xx} + ru, \quad \text{for} \quad x \in (0, L). \tag{2.5.7}$$

The equations outside $(0, L)$ can be solved explicitly, and the solutions can be used to turn the matching conditions at the interface into the mixed boundary conditions

$$u_x(0, t) = \frac{\sqrt{D_2(m+\lambda)}}{D_1 k} u(0, t), \tag{2.5.8}$$
$$u_x(L, t) = -\frac{\sqrt{D_2(m+\lambda)}}{D_1 k} u(L, t). \tag{2.5.9}$$

I will explain and use this procedure in detail several times in Chapter 4.

Since the eigenvalue appears in the boundary conditions, one cannot obtain an explicit expression of the eigenvalue in terms of model parameters. However by finding the associated eigenfunctions and applying the boundary conditions, the following transcendental equation for the dominant eigenvalue is derived:

$$\tan\left(\sqrt{\frac{r-\lambda}{D_1}}L\right) - \frac{2\sqrt{D_2(m+\lambda)}}{k\sqrt{D_1(r-\lambda)}\left(1-\frac{D_2(m+\lambda)}{D_1(r-\lambda)k^2}\right)} = 0. \tag{2.5.10}$$

Given parameters for the system, the sign of the dominant eigenvalue may be obtained using (2.5.10) by graphing the left-hand side of equation (2.5.10) as a function of $\lambda$ and determining the largest value of $\lambda$ that gives a root.

The critical patch-size, however, can be determined from the transcendental equation by setting $\lambda = 0$ and solving for $L$. One obtains

$$L^* = \sqrt{\frac{D_1}{r}}\arctan\left(\frac{2\sqrt{D_2 m}}{k\sqrt{D_1 r}\left(1-\frac{D_2 m}{D_1 r k^2}\right)}\right). \tag{2.5.11}$$

I look at the limiting cases for $k$. As $k \to \infty$, the argument of the arctangent function approaches zero and therefore $L^*$ approaches zero. This is the case of no-flux conditions; see Section 2.3. As $k \to 0$, the argument of the arctangent function approaches infinity. This time one needs to take the branch shifted upwards by $\pi$ to obtain the critical patch-size $L^* = \pi\sqrt{\frac{D_1}{r}}$ as in equation (2.2.11). This is the case of hostile boundary conditions.

## 2.6 A Moving Habitat

I switch my focus now to climate change and how its impact has been incorporated into the mathematical studies of population persistence. The first study on this subject dates back to Potapov and Lewis in 2004 [10]. I begin with the conceptually simpler model by Berestycki et al. from 2009 [3].

As indicated in the introduction, each species has its own 'climate niche', the region where the temperature is exactly right for the species to grow. Outside of the climate niche, individuals will die and the population cannot grow. One of the effects of climate change is that this niche will move towards higher latitudes and/or altitudes.

This scenario can be modelled by introducing a growth function $f$ of the form

$$f(u,x) = \begin{cases} u(r-au), & x \in (0,L), \\ -mu, & x \notin (0,L), \end{cases} \tag{2.6.1}$$

where $(0, L)$ represents the climate niche in which the population grows logistically with parameters $r, a > 0$. Outside of this niche, the population declines at rate $m$. If the climate niche moves at a constant speed, then the corresponding reaction-diffusion equation is given by

$$u_t = Du_{xx} + f(u, x - ct), \quad x \in \mathbb{R}, \quad t > 0. \tag{2.6.2}$$

At the interfaces where the definition of $f$ changes, one has to impose matching conditions. Berestycki et al. assumed that the density and flux are continuous across the interfaces.

Berestycki et al. [3] approached the analysis in a geometrical sense via phase planes. The main question they ask is whether and under what conditions a positive solution of the form

$$u(t, x) = w(x - ct) \tag{2.6.3}$$

exists. It turns out that the answer is related to the critical patch-size problem. Applying the change of variable $\xi = x - ct$ to the ansatz in (2.6.3), one obtains the equation

$$Dw_{\xi\xi} + cw_\xi + f(w, \xi) = 0, \tag{2.6.4}$$

where the growth function is now time independent. The interfaces are fixed at the locations $\xi = 0, L$.

After nondimensionalization, the equation outside the interval $\xi \in (0, L)$ takes the form

$$w_{\xi\xi} + cw_\xi - w = 0. \tag{2.6.5}$$

The characteristic roots of this equation are

$$n^\pm = -\frac{c}{2} \pm \frac{\sqrt{c^2 + 4}}{2}. \tag{2.6.6}$$

As solutions are required to be bounded as $|\xi| \to \infty$, one obtains

$$w \sim e^{n^+ \xi}, \qquad \xi < 0, \tag{2.6.7}$$

$$w \sim e^{n^- \xi}, \qquad \xi > L, \tag{2.6.8}$$

with $n^+ > 0 > n^-$.

To construct the phase portrait, equation (2.6.5) is rewritten as a system of first-order equations. With $v = w_\xi$, equation (2.6.5) is equivalent to the system

$$w_\xi = v \tag{2.6.9}$$

$$v_\xi = -cv + w. \tag{2.6.10}$$

This linear system has eigenvalues $n^\pm$ and eigenvectors given by the lines $v = n^- w$ and $v = n^+ w$. The origin is a saddle point; the direction corresponding to $n^-$ is stable,

while the one with $n^+$ is unstable. A recreation of Figure 1 of the phase plane from [3] illustrates these lines in Figure 2.1.

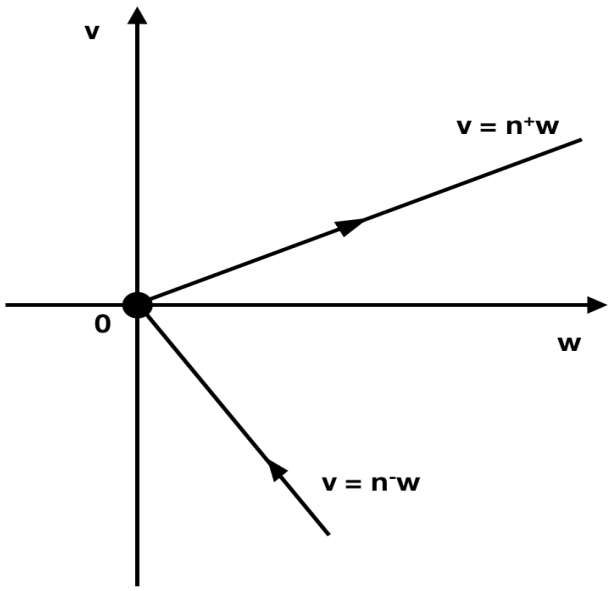


Figure 2.1: Recreation of Fig. 1 from [3]. The unstable and stable subspace (restricted to $w > 0$) for the linear system (2.6.9) – (2.6.10)

I now turn to the equation (2.6.4) in the interval $(0, L)$. After nondimensionalization, it takes the form

$$w_{\xi\xi} + cw_\xi + w(1 - w) = 0. \tag{2.6.11}$$

The equivalent first-order system is

$$w_\xi = v, \tag{2.6.12}$$
$$v_\xi = -cv - w(1 - w). \tag{2.6.13}$$

The equilibria of system (2.6.12) – (2.6.13) are $(w, v) = (0, 0)$ and $(w, v) = (1, 0)$. The eigenvalues associated with the linearization at the point $(1, 0)$ are

$$\sigma^\pm = -\frac{c}{2} \pm \frac{\sqrt{c^2 + 4}}{2}. \tag{2.6.14}$$

These eigenvalues are real with $\sigma^+ > 0 > \sigma^-$. Thus, the equilibrium $(1, 0)$ is a saddle point.

The eigenvalues associated with the linearization at the origin are

$$\sigma_0^{\pm} = -\frac{c}{2} \pm \frac{\sqrt{c^2-4}}{2}. \tag{2.6.15}$$

When $c^2 - 4 < 0$, the eigenvalues are complex conjugates so that the origin is then a stable spiral point. A recreation of Figure 2 from [3] illustrates this situation in Figure 2.2. In the case $c^2 - 4 > 0$ the eigenvalues $\sigma_0^{\pm}$ are real and negative. Hence, the origin is a stable node. This case is not illustrated since it will not yield a solution.

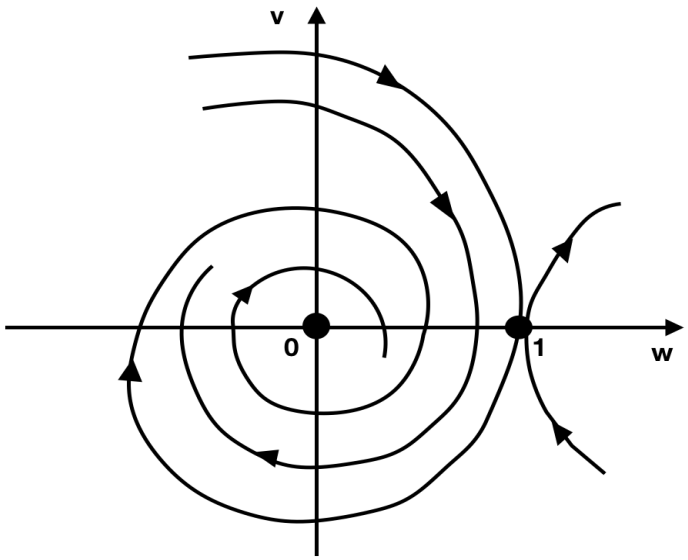


Figure 2.2: Recreation of Fig. 2 from [3]. Phase portrait of system (2.6.12) – (2.6.13) for $\left(\frac{c}{2}\right)^2 < 1$

The desired solution of (2.6.4) is a trajectory in the phase plane that starts at the origin on the line $v = n^+w$ in Figure 2.1 from $\xi \to -\infty$ until $\xi = 0$. Then it follows the trajectories in Figure 2.2 from $\xi = 0$ until $\xi = L$, when it must reach the line $v = n^-w$ from Figure 2.1. It then follows this line back to the origin as $\xi \to \infty$.

In the case $c \geq 4$, one of the eigenvectors of the nonlinear system (2.6.12) – (2.6.13) is inside the wedge created by the lines $v = n^{\pm}w$ of the linear system. Therefore, trajectories that start on the line $v = n^+w$ cannot reach the line $v = n^-w$, as the trajectory will be obstructed by the eigenvector and pulled towards the origin. For that reason, the system has no solution for $c \geq 4$.

The critical patch-size problem arises when one asks for the smallest value of $L$ for which such a desired solution exists (under the condition that $c < 4$). The smallest such $L = L^*$ is found near the origin. This result is stated and proved in [3].

Thus, $L^*$ may be found by studying system (2.6.12) – (2.6.13) linearized at the origin and subject to the boundary conditions $v(0) = n^- w(0)$ and $v(L) = n^+ w(L)$.

In much the same way as in Section 2.5, a condition for non-trivial solutions is given in terms of the model parameters as

$$\tan(\sqrt{4-c^2}L) = -\frac{4\sqrt{1+(\frac{c}{2})^2}\sqrt{1-(\frac{c}{2})^2}}{c^2}. \tag{2.6.16}$$

The critical patch-size is found by solving for $L$ and is given by

$$L^* = \frac{1}{\sqrt{4-c^2}} \arctan \frac{-4\sqrt{1+(\frac{c}{2})^2}\sqrt{1-(\frac{c}{2})^2}}{c^2}. \tag{2.6.17}$$

In Chapter 4 of my thesis, I generalize these arguments by considering the generalized boundary conditions derived in Section 2.4.

## 2.7 Two Species In A Moving Habitat

Potapov and Lewis [10] studied an extension of the model by Berestycki et al., where they considered competition between two species on a moving habitat. Their main goal was to determine how the speed with which climate change moves the species' niche affects the competitive outcome between two species.

There is a suitable bounded patch, $(L_1(t), L_2(t))$, on which two competing populations with densities $u_i(t,x)$, $i = 1, 2$, follow a reaction-diffusion equation with Lotka–Volterra competition dynamics. These equations are

$$u_{1,t} = D_1 u_{1,xx} + (r_1 - \alpha_{11}u_1 - \alpha_{12}u_2)u_1, \tag{2.7.1}$$
$$u_{2,t} = D_2 u_{2,xx} + (r_2 - \alpha_{21}u_1 - \alpha_{22}u_2)u_2, \tag{2.7.2}$$

for $L_1(t) < x < L_2(t)$ and $t > 0$. The two boundary points move at a constant speed $c$ so that the length of the patch $L_2(t) - L_1(t) = L$ remains constant.

Outside this patch, individuals die at constant rates $m_{1,2} > 0$. There is no interaction between the species. Accordingly, the equations are

$$u_{1,t} = D_1 u_{1,xx} - m_1 u_1, \tag{2.7.3}$$
$$u_{2,t} = D_2 u_{2,xx} - m_2 u_2, \tag{2.7.4}$$

for $x < L_1(t)$ and $x > L_2(t)$ and $t > 0$. At each of the interfaces, population densities $u_i$ and population fluxes $D_i u_{i,x}$ are assumed continuous.

Since the length of the bounded patch is assumed constant, the change of variable $\xi = x - ct$ fixes the bounded domain to $\xi \in (0, L)$. The result is the dynamical system

$$u_{1,t} = D_1 u_{1,\xi\xi} + c u_{1,\xi} + (r_1 - \alpha_{11}u_1 - \alpha_{12}u_2)u_1, \tag{2.7.5}$$

$$u_{2,t} = D_2 u_{2,\xi\xi} + c u_{2,\xi} + (r_2 - \alpha_{21} u_1 - \alpha_{22} u_2) u_2, \tag{2.7.6}$$

for $\xi \in (0, L)$, and

$$u_{1,t} = D_1 u_{1,\xi\xi} + c u_{1,\xi} - m_1 u_1, \tag{2.7.7}$$
$$u_{2,t} = D_2 u_{2,\xi\xi} + c u_{2,\xi} - m_2 u_2, \tag{2.7.8}$$

for $\xi \notin (0, L)$.

The system can be nondimensionalized (again using variable $x$) as follows

$$u_{1,t} = u_{1,xx} + c u_{1,x} + (1 - u_1 - \beta_{12} u_2) u_1, \tag{2.7.9}$$
$$u_{2,t} = D u_{2,xx} + c u_{2,x} + (r - \beta_{21} u_1 - u_2) u_2, \tag{2.7.10}$$

for $x \in (0, L)$, and

$$u_{1,t} = u_{1,xx} + c u_{1,x} - m_1 u_1, \tag{2.7.11}$$
$$u_{2,t} = D u_{2,xx} + c u_{2,x} - m_2 u_2, \tag{2.7.12}$$

for $x \notin (0, L)$.

Potapov and Lewis studied steady states and their stability of this nondimensionalized system. They used the technique by Ludwig et al. [8] as described in Section 2.5 to reduce the steady state problem on the infinite line to one on the bounded interval with Robin-type boundary conditions. The equations become

$$u_{1,xx} + c u_{1,x} + (1 - u_1 - \beta_{12} u_2) u_1 = 0, \qquad x \in (0, L), \tag{2.7.13}$$
$$D u_{2,xx} + c u_{2,x} + (r - \beta_{21} u_1 - u_2) u_2 = 0, \qquad x \in (0, L), \tag{2.7.14}$$
$$u_{ix} - k_i^+ u_i = 0, \qquad x = 0, i = 1, 2, \tag{2.7.15}$$
$$u_{ix} - k_i^- u_i = 0, \qquad x = L, i = 1, 2. \tag{2.7.16}$$

Here

$$k_1^{\pm} = \frac{-c \pm \sqrt{c^2 + 4m_1}}{2}, \qquad k_2^{\pm} = \frac{-c \pm \sqrt{c^2 + 4Dm_2}}{2D}, \tag{2.7.17}$$

are the roots of the characteristic equations for the associated steady state problem of equations (2.7.11) and (2.7.12).

The steady state problem (2.7.13) – (2.7.16) can be associated to a new dynamical system,

$$u_{1,t} = u_{1,xx} + c u_{1,x} + (1 - u_1 - \beta_{12} u_2) u_1 = 0, \qquad x \in (0, L), \tag{2.7.18}$$
$$u_{2,t} = D u_{2,xx} + c u_{2,x} + (r - \beta_{21} u_1 - u_2) u_2 = 0, \qquad x \in (0, L), \tag{2.7.19}$$
$$u_{ix} - k_i^+ u_i = 0, \qquad x = 0, i = 1, 2, \tag{2.7.20}$$
$$u_{ix} - k_i^- u_i = 0, \qquad x = L, i = 1, 2. \tag{2.7.21}$$

Non-stationary solutions to (2.7.18) – (2.7.21) are not equivalent to non-stationary solutions of (2.7.5) – (2.7.8). However, since the two systems coincide inside the interval $x \in (0, L)$, the stability behaviour of both systems near a steady state turns out to be identical. The following theorem on the stability of the steady states of both systems is proved by Potapov and Lewis as Theorem 3.1 in [10].

**Theorem 2.7.1.** *(Stability) Assume all model parameters are positive. Let $u^*$ be a solution of the steady state problem (2.7.13) – (2.7.13). Then $u^*$ is a steady state solution to (2.7.18) – (2.7.21) and (2.7.5) – (2.7.8). The linear stability of $u^*$ is either stable for both problems or unstable for both.*

The proof of this theorem exploits the fact that the stability of stationary solutions can be determined by the sign of the dominant eigenvalue. The eigenvalue problem corresponding to equations (2.7.5) – (2.7.8) is non-standard, as the domain is infinite; even on the bounded domain, the eigenvalue still shows up in the boundary conditions. The eigenvalue problem associated to equations (2.7.18) – (2.7.21), however, is standard. The proof introduces a parameter $l$ to take the place of the eigenvalue outside the bounded domain of the non-standard eigenvalue problem and exploits the property of the dominant eigenvalue being a continuous function of model parameters. I will extend their proof to my model with discontinuous interface conditions in Chapter 4, where I will give all the details of the proof.

The stability conditions from this theorem can now be calculated in terms of the size of the patch. Potapov and Lewis show the existence of a critical speed of the climate niche and a critical patch-size for the $i^{\text{th}}$ species in the absence of the other.

More specifically, their Proposition 4.1 states that species $i$ cannot persist for any $L > 0$ if $c > c_i^*$, which is defined as

$$c_i^* = \begin{cases} 2, & i = 1 \\ 2\sqrt{Dr}, & i = 2. \end{cases} \tag{2.7.22}$$

The interesting aspect of this observation is that $c_i^*$ are precisely the asymptotic spreading speeds of population $i$ in the absence of the other species in a homogeneously 'good' habitat [2]. The asymptotic spreading speed is the speed at which a population will eventually expand its spatial extent when introduced locally.

For $c_i < c_i^*$, Potapov and Lewis calculate the critical patch-size for persistence of the $i^{\text{th}}$ species in the absence of the other and in the limit as $m_i \to \infty$ as

$$\tilde{L}_i^* = \frac{L_i^*}{\sqrt{1 - (\frac{c}{c_i^*})^2}}, \tag{2.7.23}$$

with

$$L_i^* = \begin{cases} \pi, & i = 1 \\ \pi\sqrt{\frac{D}{r}}, & i = 2. \end{cases} \tag{2.7.24}$$

Even for finite (positive) death rates outside the climate niche, the authors can show the following asymptotic behaviour; see Proposition 4.2 in [10].

**Proposition 2.3.** *With the increase of $|c|$, the critical patch-size for the $i^{th}$ species goes to infinity as $c$ approaches $c_i^*$.*

Thus, as in [3], a finite critical patch-size is found only for $c$ less than a critical value. In terms of the original dimensional parameters for the models, this critical value is given by the famous Fisher formula for the minimal speed of a travelling wave in a homogeneous environment; i.e.,

$$c^* = 2\sqrt{D_i r_i} = 2\sqrt{Df'(0)},$$

for the models in (2.7.5) and (2.6.2), respectively.

Potapov and Lewis continue to describe the effect of the speed $c$ of the climate niche on the outcome of competition between the two species. They use numerical simulations to show that, as $c > 0$ increases, the competitive advantage shifts from the species that is locally competitively superior to the species that has the higher value of $c^*$. We return to this point in the discussion.

In this chapter, I presented the relevant mathematical literature for my thesis. In Section 2.2, I showed through a simple model on a bounded domain how the critical patch-size alone can determine the asymptotic structure of the solution to a reaction-diffusion equation describing population dynamics. Then I showed how the literature has since expanded this idea to more generalized models that include simple dynamics outside of the bounded domain, movement behaviour across interfaces and time-dependent location of interfaces. The last two additions have so far been analyzed separately. In Chapter 3, I present my model in which I combine these ideas.

# Chapter 3

# The Model

In this chapter, I present my model for a species living in a habitat that is shifting due to climate change. My model generalizes the models of Potapov and Lewis [10] and Berestycki et al. [3] by allowing the species to have a preference for a certain habitat type. As well, the assumption that mortality and diffusion rates are the same in front and behind the suitable habitat is dropped. As illustrated in the literature review, Maciel and Lutscher [9] found that this preference and difference in diffusion results in a discontinuity of density across the edges of the habitats. I use their interface conditions in my work. In contrast to Potapov and Lewis, who considered a competing species model, I consider a single species.

I start by presenting the master system consisting of three reaction-diffusion equations (RDEs) with conditions matching density and flux across each moving interface. Following Potapov and Lewis, I then scale space to fix the domain to be stationary and from there nondimensionalize the model. These steps lead to the presentation of the model that I analyze in succeeding chapters.

## 3.1 The Master Equation

I consider a single species living in a one-dimensional landscape that consists of two types of habitat. The landscape is represented by the real line, where the suitable habitat is bounded on the line by two interfaces; see Figure 3.1. The location of the interfaces is time dependent. I denote the left interface by $L_1(t)$ and the right interface by $L_2(t)$.

I denote $u = u(x,t)$ to be the population density, where $x \in \mathbb{R}$ is the spatial variable and $t \geq 0$ is the time variable. In the suitable habitat, the population dynamics are described by a semi-linear RDE. The reaction function is given by the logistic growth function with constant intrinsic growth rate, $r$, and a constant coefficient for intraspecies competition, $a$. The diffusion constant is denoted by $D$. It is assumed that movement and growth happen on the same timescale. Subscripts

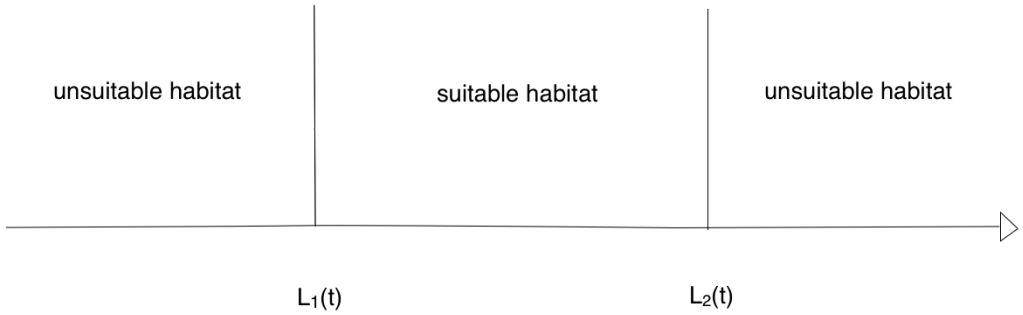


Figure 3.1: Illustration of arrangement of suitable and unsuitable habitat

are used to denote partial derivatives. Thus, the equation in the suitable habitat is

$$u_t = Du_{xx} + u(r - au), \qquad L_1(t) < x < L_2(t). \tag{3.1.1}$$

In the unsuitable habitats, the population dynamics are given by a linear RDE describing simple linear mortality and movement. I denote by $m_1$, $d_1$ the mortality rate and diffusion coefficient to the left of $L_1(t)$ and by $m_2$, $d_2$ the corresponding quantities to the right of $L_2(t)$. In the unsuitable habitats, I impose the equations

$$u_t = d_1 u_{xx} - m_1 u, \qquad x < L_1(t), \tag{3.1.2}$$
$$u_t = d_2 u_{xx} - m_2 u, \qquad x > L_2(t). \tag{3.1.3}$$

All model parameters are assumed positive.

Finally, I need to impose matching conditions at each interface. I assume that indviduals may have a preference for a habitat type. Upon reaching the interface $L_1(t)$, an individual moves to the suitable habitat with probability $\alpha$. Similarly, when reaching the interface $L_2(t)$, an individual moves to the suitable habitat with probability $\beta$.

The jump in density across each interface is measured by $k^\alpha$ and $k^\beta$, as derived in Section 2.4. Then the matching conditions for the density across each interface are

$$u(L_1^+(t), t) = k^\alpha u(L_1^-(t), t), \tag{3.1.4}$$
$$u(L_2^-(t), t) = k^\beta u(L_2^+(t), t), \tag{3.1.5}$$

with

$$k^\alpha = \frac{\alpha}{1-\alpha}\sqrt{\frac{d_1}{D}}, \qquad k^\beta = \frac{\beta}{1-\beta}\sqrt{\frac{d_2}{D}}. \tag{3.1.6}$$

Superscripts + and − denote the limit as $x$ approaches the interface from the right and left, respectively.

I also need to match the population flux across an interface in such a way that no individuals are removed or introduced as a result of movement alone. Potapov and Lewis [10] as well as Berestycki et al. [3] claimed that the population flux at an interface is $Du_x$. This is, of course, correct for a fixed interface. However, for a moving interface, the population flux changes.

To derive the appropriate expression, I consider a situation with one interface denoted by $L(t)$ on the real line. To the left of the interface, the dynamics are $u_t = d_1 u_{xx}$; to the right of the interface, the dynamics are $u_t = Du_{xx}$. When individuals are neither removed nor added at an interface, then the total density or mass does not change over time. Thus conservation of mass is expressed as

$$\frac{d}{dt}\int_{\mathbb{R}} u(x,t)dx = 0. \tag{3.1.7}$$

I calculate the integral under the condition that $u, u_x \to 0$ as $|x| \to \infty$. To simplify the calculation, I assume that the interface moves at a constant speed and thus denote $L(t) = ct$. Then the following holds,

$$\begin{aligned}
\frac{d}{dt}\int_{\mathbb{R}} u(x,t)dx &= \frac{d}{dt}\Big(\int_{-\infty}^{ct} u(x,t)dx - \int_{\infty}^{ct} u(x,t)dx\Big) \\
&= cu(ct^-,t) + \int_{-\infty}^{ct} u_t(x,t)dx - cu(ct^+,t) - \int_{\infty}^{ct} u_t(x,t)dx \\
&= cu(ct^-,t) + \int_{-\infty}^{ct} d_1 u_{xx}(x,t)dx - cu(ct^+,t) - \int_{\infty}^{ct} Du_{xx}(x,t)dx \\
&= cu(ct^-,t) + d_1 u_x(ct^-,t) - cu(ct^+,t) - Du_x(ct^+,t).
\end{aligned}$$

Hence, the correct matching condition at an interface with constant speed is

$$d_1 u_x(ct^-,t) + cu(ct^-,t) = Du_x(ct^+,t) + cu(ct^+,t). \tag{3.1.8}$$

In the models presented by Potapov and Lewis and Berestycki et al., the density was assumed to be continuous across the interface. In that case, the density terms cancel. In my model, this is not the case, as explained above.

Combining all the elements, the master system of equations is

$$\begin{cases}
u_t = Du_{xx} + u(r - au), & L_1(t) < x < L_2(t), \\
u_t = d_1 u_{xx} - m_1 u, & x < L_1(t), \\
u_t = d_2 u_{xx} - m_2 u, & x > L_2(t), \\
u(L_1^+(t),t) = k^\alpha u(L_1^-(t),t), & (Du_x + cu)(L_1^+(t),t) = (d_1 u_x + cu)(L_1^-(t),t), \\
u(L_2^-(t),t) = k^\beta u(L_2^+(t),t), & (Du_x + cu)(L_2^-(t),t) = (d_2 u_x + cu)(L_2^+(t),t), \\
L_1(t) = ct, \quad L_2(t) = L_0 + ct.
\end{cases} \tag{3.1.9}$$

This system is defined on the real line and for all times greater than zero. Initial conditions for the system give the density of the population at time $t = 0$ and are interesting only for positive densities.

## 3.2 Transforming to a Fixed Spatial Domain and Nondimensionalization

Following Potapov and Lewis [10], I fix the moving habitat with the change of variable $\xi = x - ct$. This change fixes the left and right interfaces at $\xi = 0, L_0$ and consequently fixes the suitable habitat to the interval $0 < \xi < L_0$ and the unsuitable habitats to the intervals $\xi < 0$ and $\xi > L_0$. However, the change of variables also introduces a drift term. The system on a fixed domain is

$$\begin{cases} u_t = Du_{\xi\xi} + cu_\xi + u(r - au), & 0 < \xi < L_0, \\ u_t = d_1 u_{\xi\xi} + cu_\xi - m_1 u, & \xi < 0, \\ u_t = d_2 u_{\xi\xi} + cu_\xi - m_2 u, & \xi > L_0, \\ u(0^+, t) = k^\alpha u(0^-, t), & (Du_\xi + cu)(0^+, t) = (d_1 u_\xi + cu)(0^-, t), \\ u(L_0^-, t) = k^\beta u(L_0^+, t), & (Du_\xi + cu)(L_0^-, t) = (d_2 u_\xi + cu)(L_0^+, t). \end{cases} \tag{3.2.1}$$

The system is nondimensionalized using the change of variables $X = \frac{1}{\xi_0}\xi$, $T = \frac{1}{t_0}t$, and $U = \frac{1}{u_0}u$. Applying this change to the partial differential equations in system (3.2.1) gives

$$\begin{aligned} \frac{1}{t_0}U_T &= \frac{D}{\xi_0^2}U_{XX} + \frac{c}{\xi_0}U_X + U(r - au_0 U), && 0 < X < \frac{L_0}{\xi_0}, \\ \frac{1}{t_0}U_T &= \frac{d_1}{\xi_0^2}U_{XX} + \frac{c}{\xi_0}U_X - m_1 U, && X < 0, \\ \frac{1}{t_0}U_T &= \frac{d_2}{\xi_0^2}U_{XX} + \frac{c}{\xi_0}U_X - m_2 U, && X > L_0. \end{aligned}$$

The interface conditions become

$$\begin{aligned} U(0^+, t) &= k^\alpha U(0^-, t), & \Big(\frac{D}{\xi_0}U_X + cU\Big)(0^+, t) &= \Big(\frac{d_1}{\xi_0}U_X + cU\Big)(0^-, t), \\ U\Big(\frac{L_0^-}{\xi_0}, t\Big) &= k^\beta U\Big(\frac{L_0^+}{\xi}, t\Big), & \Big(\frac{D}{\xi_0}U_X + cU\Big)\Big(\frac{L_0^-}{\xi_0}, t\Big) &= \Big(\frac{d_2}{\xi_0}U_X + cU\Big)\Big(\frac{L_0^+}{\xi_0}, t\Big). \end{aligned}$$

Choosing $\xi_0 = \sqrt{\frac{D}{r}}$, $t_0 = \frac{1}{r}$ and $u_0 = \frac{r}{a}$ gives

$$U_T = U_{XX} + \frac{c}{\sqrt{Dr}}U_X + U(1 - U), \qquad 0 < X < \frac{L_0}{\xi_0},$$

$$U_T = \frac{d_1}{D}U_{XX} + \frac{c}{\sqrt{Dr}}U_X - \frac{m_1}{r}U, \qquad X < 0,$$
$$U_T = \frac{d_2}{D}U_{XX} + \frac{c}{\sqrt{Dr}}U_X - \frac{m_2}{r}U, \qquad X > \frac{L_0}{\xi_0},$$

and, for the interface conditions,

$$U(0^+,t) = k^\alpha U(0^-,t), \qquad \Big(U_X + \frac{c}{\sqrt{Dr}}U\Big)(0^+,t) = \Big(\frac{d_1}{D}U_X + \frac{c}{\sqrt{Dr}}U\Big)(0^-,t),$$
$$U\Big(\frac{L_0^-}{\xi_0},t\Big) = k^\beta U\Big(\frac{L_0^+}{\xi},t\Big), \qquad \Big(U_X + \frac{c}{\sqrt{Dr}}U\Big)\Big(\frac{L_0^-}{\xi_0},t\Big) = \Big(\frac{d_2}{D}U_X + \frac{c}{\sqrt{Dr}}U\Big)\Big(\frac{L_0^+}{\xi_0},t\Big).$$

I now denote $L = \frac{L_0}{\xi_0}$, $D_i = \frac{d_i}{D}$, $c' = \frac{c}{\sqrt{Dr}}$, $m_i' = \frac{m_i}{r}$. I also rename the density, space and time variables, $u = U$, $x = X$ and $t = T$. Then the nondimensionalized system on a fixed spatial domain is

$$\begin{cases} u_t = u_{xx} + cu_x + u(1-u), & 0 < x < L, \\ u_t = D_1 u_{xx} + cu_x - m_1 u, & x < 0, \\ u_t = D_2 u_{xx} + cu_x - m_2 u, & x > L, \\ u(0^+,t) = k^\alpha u(0^-,t), & (u_x + cu)(0^+,t) = (D_1 u_x + cu)(0^-,t), \\ u(L^-,t) = k^\beta u(L^+,t), & (u_x + cu)(L^-,t) = (D_2 u_x + cu)(L^+,t), \end{cases} \tag{3.2.2}$$

where the primes are dropped for notational simplicity. In this notation, I now have

$$k^\alpha = \frac{\alpha}{1-\alpha}\sqrt{D_1} \quad \text{and} \quad k^\beta = \frac{\beta}{1-\beta}\sqrt{D_2}. \tag{3.2.3}$$

In this chapter, I presented my model for a population density on a moving domain. The model is suggested to capture how the population density will change in time on a bounded interval while still capturing movement behaviour outside this interval. In the next chapter, I analyze the nondimensionalized system (3.2.2). The analysis centres around the search for conditions that give stable positive solutions.

# Chapter 4

# Analysis of the Nondimensionalized Equation

In this chapter, I first set out to find the critical patch-size, $L^*$, for the model in (3.2.2). As noted in the literature review, this value depends on the dominant eigenvalue for the linearized model, which I denote by $\lambda$. Recall that the population's ability to persist relies on the sign of the dominant eigenvalue. I present a method first illustrated by Ludwig et al. [8] that reduces the eigenvalue problem on the infinite domain to one on a bounded domain. This leads to a non-standard eigenvalue problem. I then show, following Potapov and Lewis [10], that the sign of $\lambda$ for the non-standard eigenvalue problem is determined by the dominant eigenvalue for a standard eigenvalue problem.

I continue my analysis using the standard eigenvalue problem to determine the critical patch-size. In contrast to [3] and [10], I show that, for any speed $c$, I can find the existence of a finite critical patch-size. The analysis is broken into two cases. Case one demonstrates that, for any $c < 2$, $L^*$ exists. In case two, $c \geq 2$, I find a necessary condition for the existence of $L^*$. For both cases, a representation formula is given for $L^*$ by following Maciel and Lutscher [9].

## 4.1 Linearization and the Eigenvalue Problem

Here I linearize the model in (3.2.2) to obtain persistence conditions and the critical patch-size by following the steps in [9]. For $x \notin (0, L)$, the equations are already linear. I linearize the equation for $x \in (0, L)$ about low densities and obtain

$$u_t = u_{xx} + cu_x + u, \quad x \in (0, L). \tag{4.1.1}$$

I solve the linear problem using the method of separation of variables, assuming classical solutions of the form $u(x, t) = T(t)X(x)$. With this assumption, the equations reduce to the eigenvalue problem,

$$\dot{T} = \lambda T, \qquad t > 0, \tag{4.1.2}$$

$$X'' + cX' + X = \lambda X, \qquad 0 < x < L, \tag{4.1.3}$$
$$D_1 X'' + cX' - m_1 X = \lambda X, \qquad x < 0, \tag{4.1.4}$$
$$D_2 X'' + cX' - m_2 X = \lambda X, \qquad x > L. \tag{4.1.5}$$

The interface conditions in (3.2.2) translate into the following:

$$X(0^+) = k^\alpha X(0^-), \qquad (X' + cX)(0^+) = (D_1 X' + cX)(0^-), \tag{4.1.6}$$
$$X(L^-) = k^\beta X(L^+), \qquad (X' + cX)(L^-) = (D_2 X' + cX)(L^+). \tag{4.1.7}$$

This system admits exponential solutions in time; i.e., $T(t) = e^{\lambda t} T(0)$. For $x \notin (0, L)$, I have the characteristic polynomials

$$D_i n_i^2 + c n_i - (m_i + \lambda) = 0, \tag{4.1.8}$$

with roots

$$n_i^\pm = \frac{-c \pm \sqrt{c^2 + 4(m_i + \lambda) D_i}}{2 D_i}. \tag{4.1.9}$$

I impose the condition that $X \to 0$ as $|x| \to \infty$. Also, as I am concerned with the stability of the zero steady state, I assume $|\lambda| \ll 1$. With this assumption on the dominant eigenvalue, it follows that $n_i^+$ is positive and $n_i^-$ is negative. Due to the asymptotic condition and the assumption on $\lambda$, solutions outside the suitable habitat are of the form

$$X(x) \sim e^{n_1^+ x}, \qquad x < 0, \tag{4.1.10}$$
$$X(x) \sim e^{n_2^- x}, \qquad x > L. \tag{4.1.11}$$

These solutions satisfy the differential equations

$$X' = n_1^+ X, \qquad x < 0, \tag{4.1.12}$$
$$X' = n_2^- X, \qquad x > L. \tag{4.1.13}$$

Looking first at a neighbourhood of $x = 0$, I can combine the information at the interface $x = 0$ with the differential equation (4.1.12) to recover the following string of equalities,

$$\begin{aligned} X'(0^+) + cX(0^+) &= D_1 X'(0^-) + cX(0^-) && \text{(interface condition)} \\ &= D_1 n_1^+ X(0^-) + cX(0^-) && \text{(from equation (4.1.12))} \\ &= \frac{D_1 n_1^+ + c}{k^\alpha} X(0^+). && \text{(interface condition)} \end{aligned}$$

Similarly, at $x = L$, I have

$$X'(L^-) + cX(L^-) = D_2 X'(L^+) + cX(L^+) = D_2 n_2^- X(L^+) + cX(L^+) = \frac{D_2 n_2^- + c}{k^\beta} X(L^-). \tag{4.1.14}$$

With these equalities, I can now consider equation (4.1.3) on the bounded domain $x \in [0, L]$ with boundary conditions

$$X' + cX = \gamma^\alpha X, \qquad \text{at } x = 0, \tag{4.1.15}$$
$$X' + cX = \gamma^\beta X, \qquad \text{at } x = L, \tag{4.1.16}$$

where

$$\gamma^\alpha = \frac{D_1 n_1^+ + c}{k^\alpha}, \qquad \gamma^\beta = \frac{D_2 n_2^- + c}{k^\beta}. \tag{4.1.17}$$

The boundary conditions state that the flux at any point on the boundary is proportional to the density. This is a nonstandard eigenvalue problem as both $n_1^+$ and $n_2^-$ contain $\lambda$ and thus so do the boundary conditions. In the next section, I show that I can study the sign of the dominant eigenvalue for the resulting system by studying a standard eigenvalue problem instead.

## 4.2 Steady States and Their Stability

I consider stationary solutions for system (3.2.2); i.e., set $u_t = 0$. The zero state, which I considered in the previous section, is one steady state, but the theory developed here also covers nonzero steady states. Then, using the method of Ludwig et al. [8], the problem on the infinite domain may be reduced to a boundary-value problem on $[0, L]$. Similar to the procedure in the previous section, I first find solutions to the equations outside the suitable habitat. I then derive boundary conditions by connecting density and flux via the interface conditions.

On the intervals $x < 0, x > L$, solutions to the stationary problem satisfy,

$$D_i u_{xx} + c u_x - m_i u = 0, \qquad i = 1, 2. \tag{4.2.1}$$

Bounded solutions for these equations are of the form

$$u(x) \sim e^{n_0^+ x}, \qquad x < 0, \tag{4.2.2}$$
$$u(x) \sim e^{n_0^- x}, \qquad x > L, \tag{4.2.3}$$

where

$$n_0^+ = \frac{-c}{2D_1} + \frac{\sqrt{c^2 + 4D_1 m_1}}{2D_1} \quad \text{and} \quad n_0^- = \frac{-c}{2D_2} - \frac{\sqrt{c^2 + 4D_2 m_2}}{2D_2}. \tag{4.2.4}$$

For $x < 0$, $u$ satisfies the equation $u_x = n_0^+ u$. This relation, combined with the interface conditions at $x = 0$, gives the boundary condition

$$u_x(0^+) + cu(0^+) = D_1 u_x(0^-) + cu(0^-) = D_1 n_0^+ u(0^-) + cu(0^-) = \frac{D_1 n_0^+ + c}{k^\alpha} u(0^+). \tag{4.2.5}$$

Similarly, I obtain the right-hand side boundary condition

$$u_x(L^-) + cu(L^-) = \frac{D_2 n_0^- + c}{k^\beta} u(L^-). \tag{4.2.6}$$

Therefore, the system for stationary solutions on an infinite domain is reduced to the boundary value problem

$$\begin{cases} u_{xx} + cu_x + u(1-u) = 0, & 0 < x < L, \\ u_x + cu = \gamma_0^\alpha u, & x = 0, \\ u_x + cu = \gamma_0^\beta u, & x = L, \end{cases} \tag{4.2.7}$$

where

$$\gamma_0^\alpha = \frac{c + \sqrt{c^2 + 4m_1 D_1}}{2k^\alpha} \quad \text{and} \quad \gamma_0^\beta = \frac{c - \sqrt{c^2 + 4m_2 D_2}}{2k^\beta}. \tag{4.2.8}$$

Following Potapov and Lewis [10], I associate to the steady state problem (4.2.7) a new dynamical system

$$\begin{cases} u_t = u_{xx} + cu_x + u(1-u), & 0 < x < L, \\ u_x + cu = \gamma_0^\alpha u, & x = 0, \\ u_x + cu = \gamma_0^\beta u, & x = L. \end{cases} \tag{4.2.9}$$

Non-stationary solutions to system (3.2.1) are not equivalent to system (4.2.9); however, their stationary solutions coincide; see system (4.2.7). Due to this relation I can study the effects of small perturbations away from stationary solutions of both systems. The following theorem is a generalization of Theorem 3.1 in Potapov and Lewis [10], which is also stated in the literature review in section 2.7 as Theorem 2.7.1.

**Theorem 4.2.1.** *(Stability) Let $u^*(x)$ be a solution of system (4.2.7). Then $u^*(x)$ is a steady state solution for both (3.2.1) and (4.2.9). The linear stability of $u^*(x)$ is either stable for both (3.2.1) and (4.2.9) or unstable for both systems.*

Before presenting the proof, I would like to call attention to a relation between the boundary conditions and $\lambda$. The sign of $\gamma_0^\beta$ is negative, and the sign of $\gamma_0^\alpha$ is positive. Considering movement only, the change in total mass is calculated as

$$\frac{d}{dt}\int_0^L u(x,t)dx = \int_0^L u_{xx}(x,t) + cu_x(x,t)dx \tag{4.2.10}$$

$$= u_x(L,t) + cu(L,t) - u_x(0,t) + cu(0,t) \tag{4.2.11}$$

$$= \gamma_0^\beta u(L) - \gamma_0^\alpha u(0). \tag{4.2.12}$$

Since density is nonnegative, the total mass, when considering movement only, is a decreasing function in time. This implies that the flow out of the bounded domain is greater than the flow into this domain. This is sometimes called a *leaky boundary*. It gives a physical reason for why $\lambda$ is a decreasing function of $|\gamma^\beta|$ and $|\gamma^\alpha|$. This fact is proven in [4] and is summarized as a proposition in the literature review as Proposition 2.2. It will be used in the proof of Theorem 4.2.1.

**Proof:**
Denote $u^*(x)$ as a stationary solution for systems (3.2.1) and (4.2.9). Then the linearized equations for $v = u - u^*$ coincide inside the interval $(0, L)$ as well. Following Potapov and Lewis [10], I split the proof in two cases.

*Case 1:* $c = 0$. In this case, stationary equations for both (3.2.1) and (4.2.9) are governed by an elliptic, self-adjoint operator. Consequently, system (4.2.9) is known to have a principal eigenvalue that admits a positive eigenfunction as reviewed in section 2.1.

Let $f(u) = u(1-u)$. Then the eigenvalue problem associated to the linearized system of (4.2.9) is

$$\begin{cases} v_{xx} - g(x)v = \lambda v, & 0 < x < L, \\ v_x - \gamma_0^\alpha v = 0, & x = 0, \\ v_x - \gamma_0^\beta v = 0, & x = L, \end{cases} \tag{4.2.13}$$

where $g(x) = f'(u^*(x)) = 1 - 2u^*(x)$. With $c = 0$, the coefficients in the boundary condition become $\gamma_0^\alpha = \frac{\sqrt{m_1 D_1}}{k^\alpha}$ and $\gamma_0^\beta = -\frac{\sqrt{m_2 D_2}}{k^\beta}$.

The corresponding eigenvalue problem associated to the linearized, nondimensionalized system of (3.2.1) is

$$\begin{cases} v_{xx} - g(x)v = \lambda v, & 0 < x < L, \\ D_1 v_{xx} - m_1 v = \lambda v, & x < 0, \\ D_2 v_{xx} - m_2 v = \lambda v, & x > L \\ v(0^+) = k^\alpha v(0^-), \quad v_x(0^+) = D_1 v_x(0^-) & \\ v(L^-) = k^\beta v(L^+), \quad v_x(L^-) = D_2 v_x(L^+). & \end{cases} \tag{4.2.14}$$

Consider the auxiliary quasi-eigenvalue problem corresponding to (4.2.14),

$$\begin{cases} v_{xx} - g(x)v = \lambda v, & 0 < x < L, \\ D_1 v_{xx} - m_1 v = lv, & x < 0, \\ D_2 v_{xx} - m_2 v = lv, & x > L, \end{cases} \tag{4.2.15}$$

with parameter $l > \max(-m_1, -m_2)$ and interface conditions as in (4.2.14). The advantage of introducing the parameter $l$ is that, upon using the same technique seen

previously, (4.2.15) can be reduced to a system on a bounded domain, while excluding $\lambda$ from the boundary conditions. The resulting system is

$$\begin{cases} v_{xx} - g(x)v = \lambda v, & 0 < x < L, \\ v_x + B(x)v = 0 & x = 0, L, \end{cases} \tag{4.2.16}$$

where

$$B(x) = \begin{cases} -\frac{D_1 \tilde{n}^+(l)}{k^\alpha}, & \text{at} \quad x = 0, \\ -\frac{D_2 \tilde{n}^-(l)}{k^\beta}, & \text{at} \quad x = L, \end{cases} \tag{4.2.17}$$

and $\tilde{n}^+(l) = \sqrt{\frac{m_1+l}{D_1}}$ and $\tilde{n}^-(l) = -\sqrt{\frac{m_2+l}{D_2}}$. Corollary 2.2 in [4] states that the principal eigenvalue of (4.2.16) is a continuous and decreasing function of $|B|$ and therefore also of $l$. I denote this eigenvalue as $\lambda(l)$. I present in two cases that if one of the two systems (4.2.13) or (4.2.14) admits a positive eigenvalue, then so must the other.

1. I denote the principle eigenvalue of (4.2.13) as $\lambda_A$ and suppose $\lambda_A > 0$. The function $\sigma(l) = \lambda(l) - l$ is a decreasing and continuous function of $l$. I show that there exists some $l_B$ such that $0 < l_B < \lambda_A$ and $\sigma(l_B) = 0$. First, taking $l = 0$ reduces (4.2.16) to (4.2.13). Thus $\sigma(0) = \lambda(0) = \lambda_A$. Now, taking $l = \lambda_A$, I find that $\sigma(\lambda_A) = \lambda(\lambda_A) - \lambda_A < \lambda(0) - \lambda_A = 0$. So $\sigma(0) > 0 > \sigma(\lambda_A)$. Since $\sigma$ is continuous, the intermediate value theorem guarantees the existence of $l_B$ with $\sigma(l_B) = 0$, which implies $\lambda(l_B) = l_B$. Thus, for $l = l_B$, the system (4.2.15) is identical to (4.2.14), and I can conclude that there exists a positive eigenvalue $l_B$ of (4.2.14). Consequently, given a positive principal eigenvalue for (4.2.13), system (4.2.14) also admits a positive eigenvalue.

2. Now suppose that system (4.2.14) has a positive principal eigenvalue $\lambda_B > 0$. Taking $l = \lambda_B$ implies that (4.2.16) has at least one positive eigenvalue, namely $\lambda_B$; in particular, its principal eigenvalue is then also positive. I now take $l = 0$. As $\lambda(l)$ is a decreasing function of $l$, I claim that $\lambda_A$ is also positive. Indeed, $\lambda_A = \lambda(0) > \lambda(l_B) \geq \lambda_B > 0$. Thus, given a positive principal eigenvalue for (4.2.14), system (4.2.13) also admits a positive principal eigenvalue.

*Case 2:* $c > 0$. When $c$ is non-zero, the operator governing these equations is no longer self-adjoint, and Corollary 2.2 in [4] does not apply directly. However, following Chapter 2 of [4], I can transform the system with a change of variable so that the theory applies. With non-zero $c$, the eigenvalue problems that I want to compare are

$$\begin{cases} v_{xx} + cv_x - g(x)v = \lambda v, & 0 < x < L, \\ v_x + cv = \gamma_0^\alpha v, & x = 0, \\ v_x + cv = \gamma_0^\beta v, & x = L, \end{cases} \tag{4.2.18}$$

and

$$\begin{cases} v_{xx} + cv_x - g(x)v = \lambda v, & 0 < x < L, \\ D_1 v_{xx} + cv_x - m_1 v = lv, & x < 0, \\ D_2 v_{xx} + cv_x - m_2 v = lv, & x > L, \\ v(0^+) = k^\alpha v(0^-), \qquad (v_x + cv)(0^+) = (D_1 v_x + cv)(0^-), & \\ v(L^-) = k^\beta v(L^+), \qquad (v_x + cv)(L^-) = (D_2 v_x + cv)(L^+). & \end{cases} \tag{4.2.19}$$

The eigenvalue problem in (4.2.19) is analogous to equations (4.1.3) –(4.1.5) with interface conditions (4.1.7) and (4.1.6). Thus, after the same transformation as above, system (4.2.19) is equivalent to the eigenvalue problem on the bounded domain

$$\begin{cases} v_{xx} + cv_x - g(x)v = \lambda v, & 0 < x < L, \\ v_x + cv = \gamma^\alpha(l)v, & x = 0, \\ v_x + cv = \gamma^\beta(l)v, & x = L, \end{cases} \tag{4.2.20}$$

with

$$\gamma^\alpha(l) = \frac{D_1 n_1(l)^+ + c}{k^\alpha}, \quad \gamma^\beta = \frac{D_2 n_2^-(l) + c}{k^\beta}, \quad \text{and} \quad n_i^\pm(l) = \frac{-c \pm \sqrt{c^2 + 4(m_i + l)D_i}}{2D_i}.$$

I then make the change of variable $w = ve^{cx}$ to transform the advective term in the boundary conditions. Then systems (4.2.18) and (4.2.20) become

$$\begin{cases} w_{xx} - cw_x - g(x)w = \lambda w, & 0 < x < L, \\ w_x = \gamma_0^\alpha w, & x = 0, \\ w_x = \gamma_0^\beta w, & x = L, \end{cases} \tag{4.2.21}$$

and

$$\begin{cases} w_{xx} - cw_x - g(x)w = \lambda w, & 0 < x < L, \\ w_x = \gamma^\alpha(l)w, & x = 0, \\ w_x = \gamma^\beta(l)w, & x = L. \end{cases} \tag{4.2.22}$$

Next, to transform the advective term in the interval $(0, L)$, I multiply the differential equation by $e^{-cx}$ and note that

$$(e^{-cx}w_x)_x = e^{-cx}w_{xx} - ce^{-cx}w_x = e^{-cx}(w_{xx} - cw_x).$$

I thus obtain the two systems

$$\begin{cases} (e^{-cx}w_x)_x - g(x)e^{-cx}w = \lambda e^{-cx}w, & 0 < x < L, \\ e^{-cx}w_x - \gamma_0^{\alpha}e^{-cx}w = 0, & x = 0, \\ e^{-cx}w_x - \gamma_0^{\beta}e^{-cx}w = 0, & x = L, \end{cases} \tag{4.2.23}$$

and

$$\begin{cases} (e^{-cx}w_x)_x - g(x)e^{-cx}w = \lambda e^{-cx}w, & 0 < x < L, \\ e^{-cx}w_x - B(x)e^{-cx}w = 0, & x = 0, L, \end{cases} \tag{4.2.24}$$

where

$$B(x) = \begin{cases} -\gamma^{\alpha}(l), & \text{at} \quad x = 0, \\ -\gamma^{\beta}(l), & \text{at} \quad x = L. \end{cases} \tag{4.2.25}$$

Since $e^{-cx}$ is strictly positive, systems (4.2.23) and (4.2.24) are governed by an elliptic, self-adjoint operator so that the theory from Case 1 can be applied. Since $|B(x)|$ is a increasing function of $l$, the results from the first case are valid. ∎

In this section, I showed that I can now study system (4.2.9) to obtain persistence results for system (3.2.1). This connection between the two systems simplifies the analysis by ridding any complexities that arise from the nonstandard eigenvalue problem associated with system (3.2.1).

## 4.3 The Critical Patch-Size

In this section, I calculate the critical patch-size. I take $\lambda = 0$, since this value marks the bifurcation between population persistence and extinction. I work now with the bounded system (4.2.9), as, in the previous section, it was shown that persistence conditions for system (4.2.9) are equivalent to persistence conditions for system (3.2.1). As a nonzero solution implies that the zero-equilibrium is unstable, I start by linearizing around $u = 0$.

System (4.2.9) linearized near $u = 0$ is

$$\begin{cases} u_t = u_{xx} + cu_x + u, & 0 < x < L, \\ u_x + cu = \gamma_0^{\alpha}u, & x = 0, \\ u_x + cu = \gamma_0^{\beta}u, & x = L. \end{cases} \tag{4.3.1}$$

To simplify the boundary conditions, I make the change of variable $v = ue^{cx}$ and arrive at

$$\begin{cases} v_t = v_{xx} - cu_x + v, & 0 < x < L, \\ v_x = \gamma_0^\alpha v, & x = 0, \\ v_x = \gamma_0^\beta v, & x = L. \end{cases} \tag{4.3.2}$$

As in Section 4.1, the eigenvalue problem is set up by assuming $u(x,t) = T(t)X(x)$. This assumption gives $T(t) = e^\lambda t$ for all $t \geq 0$. $X$ then satisfies

$$X'' - cX' + X = \lambda X, \qquad 0 < x < L, \tag{4.3.3}$$

$$X' = \gamma_0^\alpha X, \qquad x = 0, \tag{4.3.4}$$

$$X' = \gamma_0^\beta X, \qquad x = L. \tag{4.3.5}$$

When $\lambda = 0$, the characteristic polynomial for equation (4.3.3) is

$$n_0^2 - cn_0 + 1 = 0, \tag{4.3.6}$$

with roots

$$n_0^\pm = \frac{c}{2} \pm \frac{\sqrt{c^2 - 4}}{2}. \tag{4.3.7}$$

Thus, solutions are $X(x) = Ae^{n_0^+} + Be^{n_0^-}$, where coefficients $A, B$ are determined by the boundary conditions. I need to find conditions on model parameters, in particular $L$, such that a non-trivial solution exists. The analysis will now be broken up into two cases.

### 4.3.1 Case 1: A negative radicand

When $c < 2$, the radicand in (4.3.7) is negative. I will use phase-plane analysis to show that one can always choose $L$ so that a non-trivial solution to (4.3.3)–(4.3.5) exists. Then I will give an explicit expression for this critical domain size $L$.

The second-order problem in (4.3.3) is equivalent to

$$Y = X', \qquad Y' = X'' = -X + cY.$$

A solution that satisfies the boundary conditions corresponds to a trajectory in the $(X, Y)$-phase plane that starts on the positively-sloped line $Y = \gamma_0^\alpha X$ and reaches the negatively sloped line $Y = \gamma_0^\beta X$ in an $x$-interval of exactly length $L$. To find such trajectories, I start by looking at the Jacobian for this system, which is

$$J = \begin{bmatrix} 0 & 1 \\ -1 & c \end{bmatrix}. \tag{4.3.8}$$

I calculate $\det(J) = 1$ and the $\mathrm{Tr}(J) = c$. Thus, the eigenvalues for $J$ are

$$\sigma^{\pm} = \frac{c}{2} \pm \frac{\sqrt{c^2 - 4}}{2}. \tag{4.3.9}$$

As $c < 2$, these eigenvalues are strictly complex and have positive real part, $\Re(\sigma^{\pm}) = \frac{c}{2}$. Thus, the origin is an unstable focus. Due to the underlying vector field, orbits spiral in a clockwise direction. The quadrants of interest in the phase plane are quadrants one and four. Thus, trajectories starting in the first quadrant on the line $Y = \gamma_0^{\alpha} X$ will spiral and reach the line $Y = \gamma_0^{\beta} X$. See Figure 4.1 for an illustration of the phase portrait.

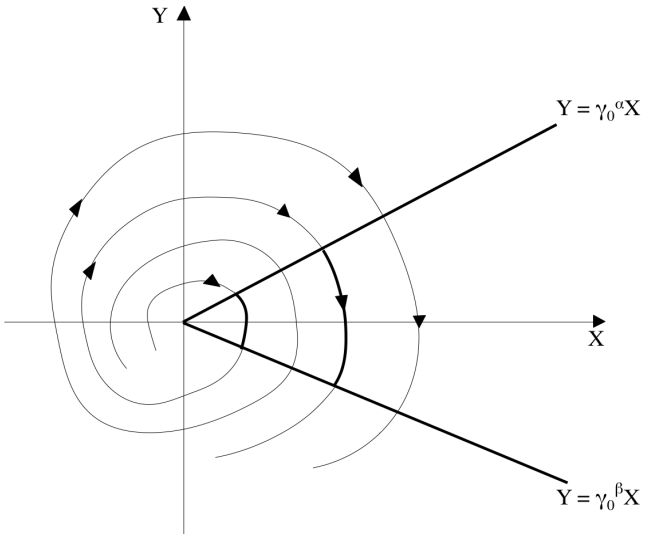


Figure 4.1: Phase portrait for $c < 2$

Going back to the linearized problem (4.3.3)–(4.3.5), the characteristic roots may be written as

$$n_0^{\pm} = \frac{c}{2} \pm i z_0, \tag{4.3.10}$$

where $z_0 = \frac{\sqrt{4-c^2}}{2}$. Solutions are then linear combinations of sine and cosine,

$$X(x) = e^{\frac{c}{2}x}\big[A_1 \cos(z_0 x) + A_2 \sin(z_0 x)\big]. \tag{4.3.11}$$

To solve for the coefficients $A_1$ and $A_2$, I apply the boundary conditions (4.3.4) and

(4.3.5) and obtain the system of two variables

$$\begin{cases} A_1(\frac{c}{2}-\gamma_0^\alpha)+A_2z_0=0 \\ A_1\big[(\frac{c}{2}-\gamma_0^\beta)\cos(z_0L)-z_0\sin(z_0L)\big]+A_2\big[(\frac{c}{2}-\gamma_0^\beta)\sin(z_0L)+z_0\cos(z_0L)\big]=0. \end{cases} \tag{4.3.12}$$

For a nontrivial solution, the determinant of the coefficient matrix of system (4.3.12) must be zero. The determinant is zero if

$$\sin(z_0L)\left[z_0^2+\left(\frac{c}{2}-\gamma_0^\alpha\right)\left(\frac{c}{2}-\gamma_0^\beta\right)\right]=\cos(z_0L)z_0(\gamma_0^\alpha-\gamma_0^\beta). \tag{4.3.13}$$

This condition may be written in terms of the tangent function as

$$\tan(z_0L)=\frac{z_0(\gamma_0^\alpha-\gamma_0^\beta)}{z_0^2+\left(\frac{c}{2}-\gamma_0^\alpha\right)\left(\frac{c}{2}-\gamma_0^\beta\right)}, \tag{4.3.14}$$

whenever $z_0^2+\left(\frac{c}{2}-\gamma_0^\alpha\right)\left(\frac{c}{2}-\gamma_0^\beta\right)\neq 0$. The critical patch-size $L^*$ is determined from condition (4.3.14) by solving for $L$. Thus, the representation formula for the critical patch-size is

$$L^*_{c<2}=\frac{1}{z_0}\arctan\left(\frac{z_0(\gamma_0^\alpha-\gamma_0^\beta)}{z_0^2+\left(\frac{c}{2}-\gamma_0^\alpha\right)\left(\frac{c}{2}-\gamma_0^\beta\right)}\right). \tag{4.3.15}$$

Whenever $L\geq L^*_{c<2}$, the dominant eigenvalue $\lambda$ will be positive and the zero steady state is unstable. However, when $L<L^*_{c<2}$, the dominant eigenvalue $\lambda$ will be negative and the zero steady state is stable.

For numerical calculations, it is advantageous to evaluate condition (4.3.13) in order to avoid erroneous results when the denominator in (4.3.15) becomes zero.

### 4.3.2 Case 2: A positive radicand

Now I consider the second case when the radicand is positive; i.e., $c\geq 2$. As before, I first use a geometric argument to find conditions under which non-trivial solutions to (4.3.3)–(4.3.5) exist. Then I calculate the corresponding critical size.

The equations for the vector field in the phase plane are the same as in the previous case. With the assumption $c\geq 2$, the eigenvalues $\sigma^\pm$ are real and positive with $\sigma^+\geq\sigma^-$. Thus, the origin is an unstable node. The eigenvectors define the lines $Y=\sigma^\pm X$. Trajectories that approach these lines will follow them out to infinity. When $c=2$, the eigenvectors define the one line $Y=X$.

In the first quadrant below the line defined by $Y=\sigma^-X$, the vector field has directions $X'>0$ and $Y'<0$. In the fourth quadrant, the direction of the $X$-component changes to $X'<0$, but the direction in the $Y$-component remains the

same. Hence, trajectories that start in the first quadrant below $Y = \sigma^- X$, will eventually reach the axis $Y = 0$ with $X > 0$ and from there will eventually reach the line $X = 0$ with $Y < 0$.

The steepness of the boundary condition $Y = \gamma_0^\alpha X$ may be controlled by the parameter $k^\alpha$. Thus, for any fixed $c \geq 2$, I can choose $k^\alpha$ such that the boundary condition lies above or below the line $Y = \sigma^- X$. The former condition does not allow for a trajectory starting on the line $Y = \gamma_0^\alpha X$ to reach the line $Y = \gamma_0^\beta X$. As illustrated in Figure 4.2, the path of a trajectory is obstructed by at least one of the eigenvectors. The latter condition does allow a trajectory to pass from one boundary condition to the other; see Figure 4.3.

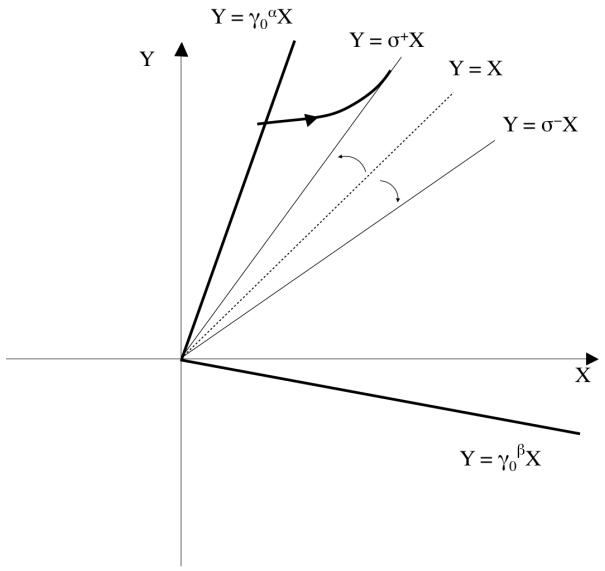


Figure 4.2: Phase portrait for $c \geq 2$ with no connection. The small arrows between the lines $Y = X$ and $Y = \sigma^{\pm}$X indicate the direction these lines would shift as $|\sigma^{\pm}|$ increases.

The necessary condition for the existence of a solution of the eigenvalue problem (4.3.3) – (4.3.5) is then

$$\gamma_0^\alpha = \frac{c + \sqrt{c^2 + 4m_1 D_1}}{2k^\alpha} < \frac{c - \sqrt{c^2 - 4}}{2} = \sigma^-. \tag{4.3.16}$$

This condition can be formulated in terms of $k^\alpha$ as

$$k^\alpha > \bar{k}^\alpha = \frac{c + \sqrt{c^2 + 4m_1 D_1}}{c - \sqrt{c^2 - 4}} > 1 + \sqrt{1 + m_1 D_1} > 2. \tag{4.3.17}$$

I summarize these considerations in terms of the critical patch-size as follows.

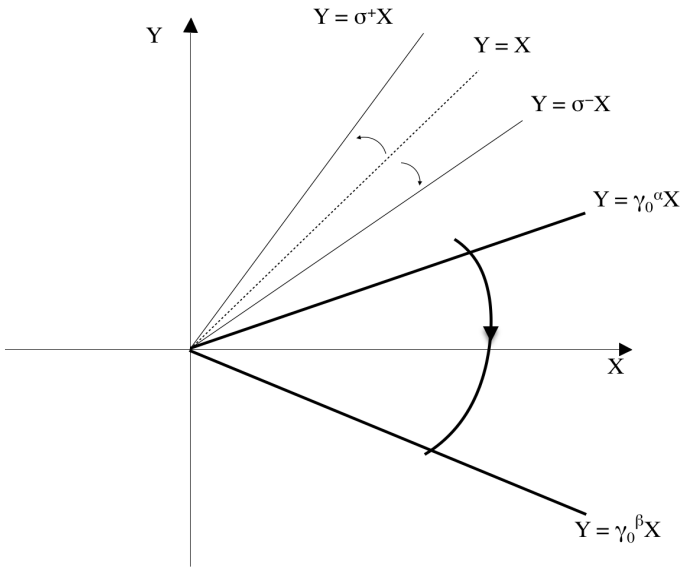


Figure 4.3: Phase portrait for $c \geq 2$ with connection. The small arrows between the lines $Y = X$ and $Y = \sigma^{\pm}$X indicate the direction these lines would shift as $|\sigma^{\pm}|$ increases.

**Theorem 4.3.1.** *(Existence of a Critical Patch-Size for $c \geq 2$) For all $c \geq 2$, there exists a $k^{\alpha}$ as in (4.3.17) such that, for all $k^{\beta} > 0$, a finite critical patch-size $L^* = L^*(c, k^{\alpha}, k^{\beta})$ exists.*

For an explicit representation formula of $L^*$ in the case $c \geq 2$, I write solutions to the linearized problem as combinations of hyperbolic sine and cosine as

$$X(x) = e^{\frac{c}{2}x}\big[A_1 \cosh(s_0 x) + A_2 \sinh(s_0 x)\big] \tag{4.3.18}$$

with $s_0 = \frac{\sqrt{c^2-4}}{2}$. To solve for $A_1$ and $A_2$, I apply the boundary conditions and obtain the linear system

$$\begin{cases} A_1(\frac{c}{2} - \gamma_0^{\alpha}) + A_2 s_0 = 0 \\ A_1\big[(\frac{c}{2} - \gamma_0^{\beta})\cosh(s_0 L) + s_0 \sinh(s_0 L)\big] + A_2\big[(\frac{c}{2} - \gamma_0^{\beta})\sinh(s_0 L) + s_0 \cosh(s_0 L)\big] = 0. \end{cases} \tag{4.3.19}$$

This system has a nontrivial solution under the condition

$$\sinh(s_0 L)\left[s_0^2 + \left(\gamma_0^{\beta} - \frac{c}{2}\right)\left(\frac{c}{2} - \gamma_0^{\alpha}\right)\right] = \cosh(s_0 L) s_0 (\gamma_0^{\beta} - \gamma_0^{\alpha}). \tag{4.3.20}$$

This condition may be written in terms of the hyperbolic tangent function as

$$\tanh(s_0 L) = \frac{s_0(\gamma_0^\beta - \gamma_0^\alpha)}{s_0^2 + \left(\gamma_0^\beta - \frac{c}{2}\right)\left(\frac{c}{2} - \gamma_0^\alpha\right)}, \tag{4.3.21}$$

provided that the denominator does not vanish. From condition (4.3.21), I obtain the representation formula for the critical patch-size to be

$$L^*_{c\geq 2} = \frac{1}{s_0} \operatorname{arctanh}\left(\frac{s_0(\gamma_0^\beta - \gamma_0^\alpha)}{s_0^2 + \left(\gamma_0^\beta - \frac{c}{2}\right)\left(\frac{c}{2} - \gamma_0^\alpha\right)}\right), \qquad k^\alpha > \bar{k}^\alpha. \tag{4.3.22}$$

In this chapter, I gave persistence conditions for system (3.1.9) and explicit formulas for $L^*$. I did so by reducing the problem on the infinite mobile domain to a problem on a bounded fixed domain with Robin-type boundary conditions. I found that, given any speed of the domain, a critical patch-size may be found. The value $c = 2$ constitutes a threshold value: when $c < 2$, there is a finite critical patch-size for any parameter values; when $c \geq 2$, a finite critical patch-size exists only when $k^\alpha$ is large enough. Thus, movement behaviour at the trailing edge of the mobile domain plays a crucial role in the asymptotic behaviour of solutions. In the next chapter, I will look at the critical patch-size as a function of model parameters.

# Chapter 5

# Illustrating The Critical Patch-Size

In this chapter, I illustrate how the critical patch-size that I calculated in the previous chapter depends on parameter values. Throughout, I concentrate on the significance of the interface conditions and on the influence of the diffusion coefficients. According to the analysis in the previous chapter, I divide the illustrations between the two cases of $c < 2$ and $c \geq 2$.

## 5.1 Case 1: The Critical Patch-Size for $c < 2$

### 5.1.1 The Critical Patch-Size as a Function of $D_1$ and $D_2$

I start by looking at the effects of the diffusion coefficient in the interval $x < ct$, or equivalently $x < 0$, after the variable change that fixes the domain; i.e., 'behind' the suitable interval; see Figure 3.1. I let $\alpha = \beta = 0.5$, so that the discontinuity of the density across the interface is introduced only due to diffusion rates.

According to the graphs in Figure 5.1, the critical patch-size is a decreasing function of $D_1$. In the associated bounded problem (4.3.2), increasing $D_1$ decreases $\gamma_0^\alpha$, as defined in (4.2.8). Thus, at the boundary $x = 0$, higher values of $D_1$ correspond to a lower net flux of particles out of the domain, while lower values of $D_1$ correspond to a higher flux. Therefore, the critical size decreases with $D_1$.

I also observe that $L^*_{c<2}$ is more sensitive to $D_1$ when $c$ is larger. With this, I mean that the absolute value of the slope (sometimes called sensitivity)

$$\left| \frac{dL^*_{c<2}}{dD_1} \right| \tag{5.1.1}$$

is increasing in $c < 2$. For fixed $c < 2$, the sensitivity of $L^*_{c<2}$ with respect to $D_1$ decreases as $D_1$ increases. Both of these observations can be explained by the boundary conditions as before. In particular, $\gamma_0^\alpha$ is monotone decreasing in $D_1$ for each

fixed $c > 0$ and approaches $\sqrt{m_1}$ in the limit as $D_1 \to \infty$. As a function of $c$, $\gamma_0^\alpha$ is increasing and the slope decreases with $D_1$.

For a biological interpretation, I consider a randomly moving individual in the unsuitable habitat behind the trailing edge. If the interface moves fast and the individual moves slowly, then the individual will be further away from the suitable habitat over time and hence less likely to reach that habitat again. Thus, the critical patch-size is largest for small diffusion rates behind the trailing edge. Therefore, in a fast-moving climate niche, high diffusion behind the trailing edge increases the likelihood of persistence.

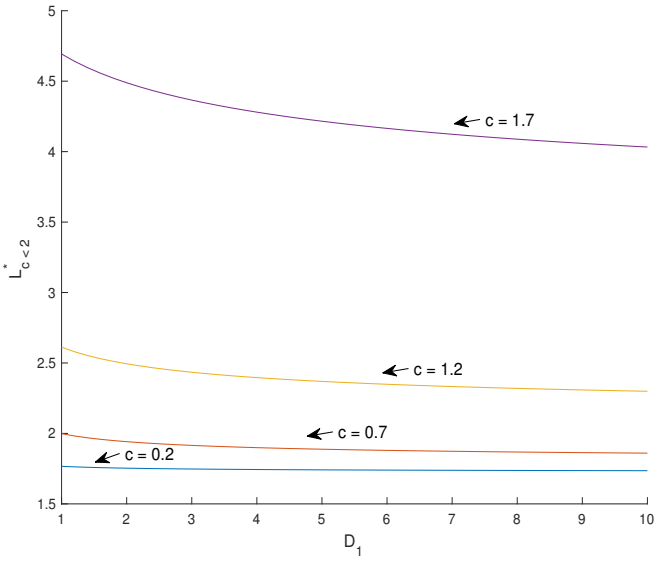


Figure 5.1: $L^*_{c<2}$ as a function of the parameter $D_1$. Model parameters are set to be $m_1 = m_2 = 1.4$, $D_2 = 2$ and $\alpha = \beta = 0.5$.

Now I look at the parameter $D_2$, the diffusion rate in the interval $x > L_0 + ct$ (or $x > L$ in the fixed domain); i.e,. 'ahead' of the suitable patch. Again, I fix $\alpha = \beta = 0.5$.

The illustration in Figure 5.2 shows that $L^*_{c<2}$ is an increasing function of $D_2$. For an explanation, I look again at the associated bounded problem (4.3.2). As before, $\gamma_0^\beta$ is monotone decreasing with respect to $D_2$, but, since it is negative, its absolute value is increasing and therefore the net flux out of the domain is increasing, which leads to a higher value of $L^*_{c<2}$. As before, $L^*_{c<2}$ is more sensitive to $D_2$ when $c$ is larger and less sensitive when $D_2$ is larger.

For a biological interpretation, I consider a randomly moving individual ahead of the leading edge of the suitable habitat. As the individual moves faster, it can

move further away from the leading edge in a shorter amount of time. However, as the interfaces are moving towards the individual, slow-moving individuals are easily swept back into the domain. Accordingly, if individuals move quickly ahead of the front, the length of the critical patch-size increases. Persistence is more likely if individuals move slowly ahead of the suitable patch.

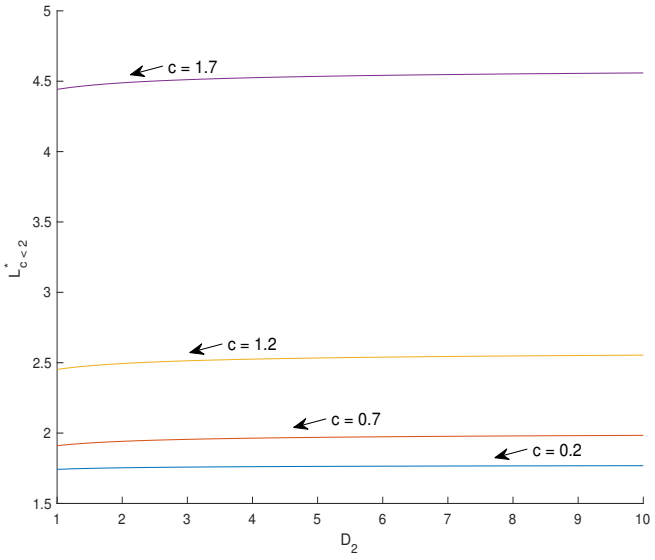


Figure 5.2: $L^*_{c<2}$ as a function of the parameter $D_2$. Model parameters are set to be $m_1 = m_2 = 1.4$, $D_1 = 2$ and $\alpha = \beta = 0.5$.

### 5.1.2 The Critical Patch-Size as a Function of $\alpha$ and $\beta$

Now I look at the effects of parameters $\alpha, \beta$; i.e., the probability that an individual at the left-hand or right-hand interface will choose to move into the suitable habitat. I set $D_1 = D_2 = 1$ so the discontinuity in density across an interface is caused only by the parameters $\alpha$ at $x = ct$ (or $x = 0$) and $\beta$ at $x = L_0 + ct$ (or $x = L$).

The plots in Figures 5.3 (for $\beta = 0.9$) and 5.4 (for $\beta = 0.1$) show that $L^*_{c<2} = L^*_{c<2}(\alpha)$ is a decreasing function of $\alpha$, all other parameters being fixed. This behaviour can be explained by looking at the boundary conditions again. At the trailing end, we have

$$(Du_x + cu) = \gamma_0^\alpha u,$$

so that the flux is proportional to the density. The parameter $\alpha$ appears in the denominator of $\gamma_0^\alpha$ since $k^\alpha = \frac{\alpha}{1-\alpha}\sqrt{D_1}$. Thus, large values of $\alpha$ correspond to a small flux, approaching a Neumann-type boundary condition in the limit $\alpha \to 1$. Small

values of $\alpha$ give large values of $\gamma_0^\alpha$ and thereby approach a Dirichlet-type condition in the limit as $\alpha \to 0$. Similarly, at the boundary $x = L$, large values of $\beta$ correspond closely to Neumann-type conditions. Small values of $\beta$ correspond closely to Dirichlet-type conditions.

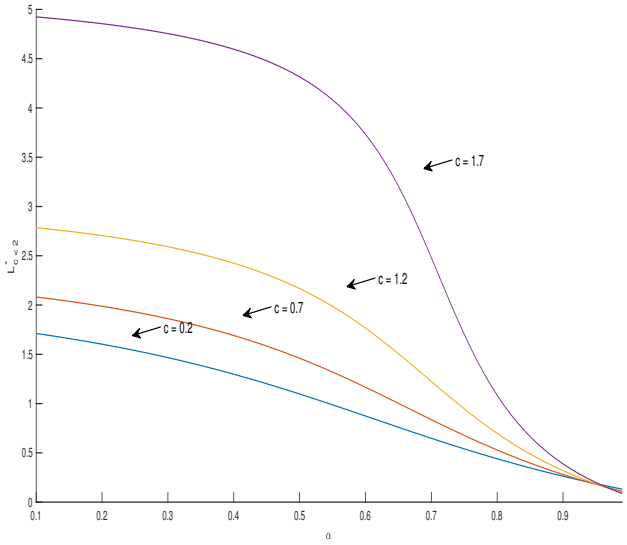


Figure 5.3: $L^*_{c<2}$ as a function of the parameter $\alpha$. Model parameters are set to be $m_1 = m_2 = 1.4$, $D_1 = D_2 = 1$ and $\beta = 0.9$.

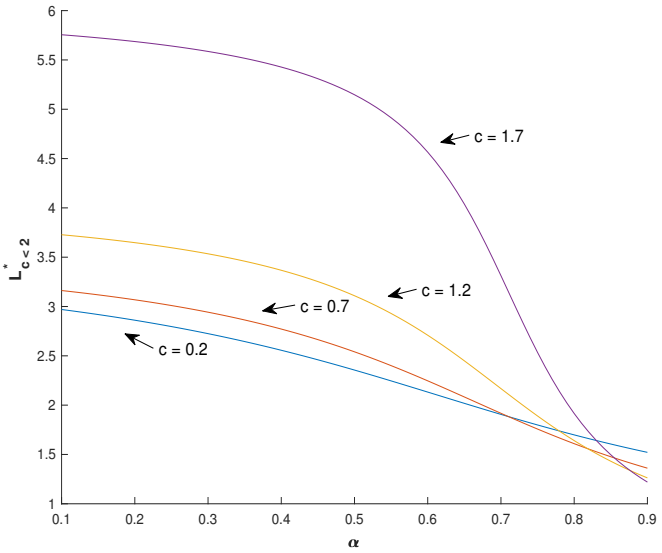


Figure 5.4: $L^*_{c<2}$ as a function of the parameter $\alpha$. Model parameters are set to be $m_1 = m_2 = 1.4$, $D_1 = D_2 = 1$ and $\beta = 0.1$.

The biological interpretation of the result is fairly obvious: as $\alpha$ increases, individuals have a higher probability to stay within the suitable patch at the trailing end, the likelihood of persistence is higher, and hence the critical patch-size is smaller.

I also note that $L^*_{c<2}$ is more sensitive to changes in $\alpha$ when $c$ is larger. For fixed $c$, however, the sensitivity with respect to $\alpha$ is greatest for intermediate values of $\alpha$.

The somewhat surprising observation is that $L^*_{c<2}$ is not monotone increasing in $c$ (for fixed $\alpha$). The curves corresponding to different values of $c$ cross as $\alpha$ increases. The intersection for large $\beta$ occurs for values of $\alpha$ much closer to unity. For a close up of these intersections please see Figure 5.5. As well, I observe that larger values of $\beta$ result in smaller critical domain sizes.

To explain this observation, I note that the parameter $c$ affects $\gamma_0^\alpha$ as well as $\gamma_0^\beta$. Both values increase with $c$, but since $\gamma_0^\alpha$ is positive and $\gamma_0^\beta$ is negative (see Figure 5.6), this means that, while $|\gamma_0^\alpha|$ is increasing, and with it the net flux from the domain at $x = 0$, $|\gamma_0^\beta|$ is decreasing, and with it the net flux from the domain at $x = L$. The total loss from the domain is the sum of the losses through each interface. When $\beta$ is large, the sensitivity of $\gamma_0^\beta$ with respect to $c$ is minimal (see Figure 5.6), and the increase in $\gamma_0^\alpha$ leads to the increased critical domain size. When $\beta$ is small, then $|\gamma_0^\beta|$ decreases significantly with $c$ (see Figure 5.6) so that the critical domain size decreases when $\alpha$ is fixed close to unity.

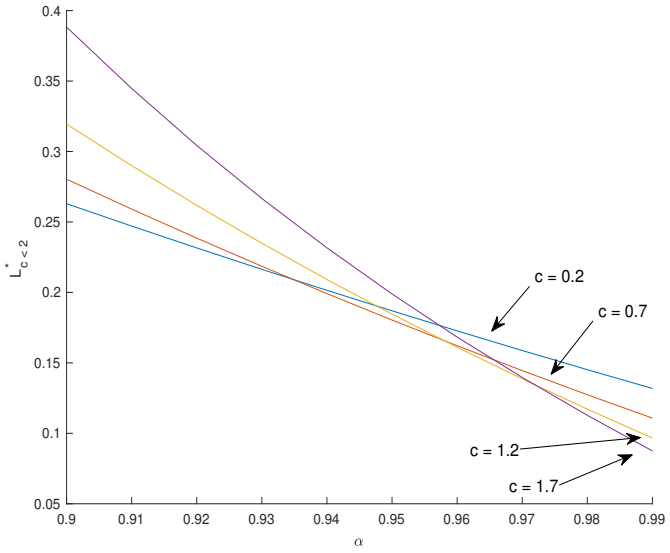


Figure 5.5: A close up of $L^*_{c<2}$ as a function of the parameter $\alpha$ on the intersection of the plots. Model parameters are set to be $m_1 = m_2 = 1.4$, $D_1 = D_2 = 1$ and $\beta = 0.1$.

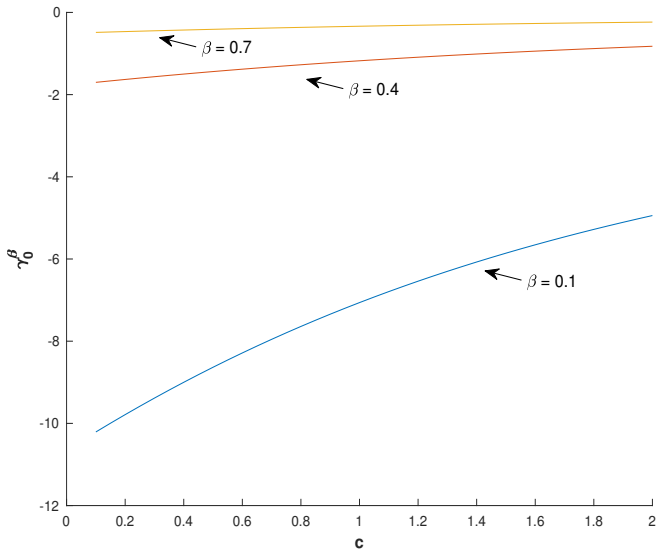


Figure 5.6: $\gamma_0^\beta$ as a function of the parameter $c$. Model parameters are set to be $m_2 = 1.4$, $D_2 = 1$.

For a biological interpretation, I consider an individual at the leading edge of the suitable habitat. If $\beta$ is large, then this individual is highly likely to stay in the suitable habitat, no matter how fast the habitat moves. The loss of individuals from the suitable habitat happens at the trailing end where a faster speed incurs a higher loss so that the critical patch-size increases with $c$. On the other hand, if $\beta$ is small, then the individual at the leading edge is likely to leave the suitable patch. If the patch moves slowly, then the individual will move away and not return to the patch. If the patch moves fast, it is likely to catch up with the randomly moving individual and 'scoop it up' again. Even though the individual tries to leave ($\beta$ small) it cannot get away from the patch ($c$ large) and therefore is not lost from the domain. Consequently, the critical size is small.

## 5.2 Case 2: The Critical Patch-Size for $c \geq 2$

Now I consider the case where $c \geq 2$ and look at $L^*_{c\geq 2}$ as a function of model parameters. The critical patch-size is finite only if the condition in (4.3.17) holds; i.e., if

$$k^\alpha > \frac{c + \sqrt{c^2 + 4m_1 D_1}}{c - \sqrt{c^2 - 4}}. \tag{5.2.1}$$

This inequality can be re-written as a lower bound for $\alpha$ as

$$\alpha > \alpha^* = \frac{I}{I+1}, \quad \text{with} \quad I = \frac{c + \sqrt{c^2 + 4m_1 D_1}}{\sqrt{D_1}(c - \sqrt{c^2 - 4})}. \tag{5.2.2}$$

As before, I illustrate two different scenarios, one with a high and one with a low value for $\beta$. The resulting Figures 5.7 and 5.8 both demonstrate that $L^*_{c\geq 2}$ is a decreasing function of $\alpha$. The explanation is the same as in the previous section: as $\alpha$ increases, fewer individuals leave the domain at the trailing edge, and therefore the population requires less space to persist.

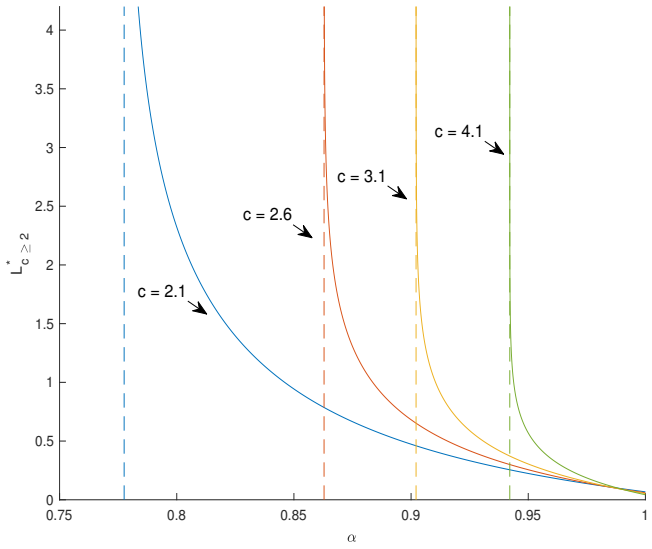


Figure 5.7: $L^*_{c\geq 2}$ as a function of the parameter $\alpha$. Model parameters are set to be $m_1 = m_2 = 1.4$, $D_1 = 1.1$, $D_2 = 2$ and $\beta = 0.9$. The solid lines are the plot of $L^*_{c\geq 2} = L^*_{c\geq 2}(\alpha)$. The dashed lines are the critical value $\alpha = \alpha^*$.

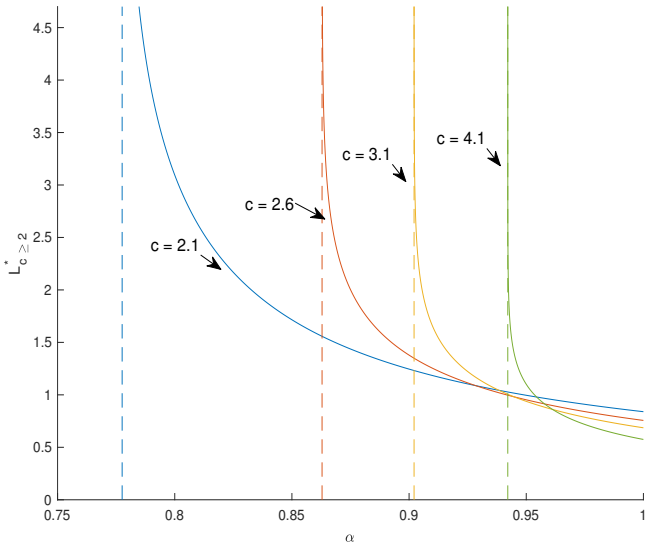


Figure 5.8: $L^*_{c\geq 2}$ as a function of the parameter $\alpha$. Model parameters are set to be $m_1 = m_2 = 1.4$, $D_1 = 1.1$, $D_2 = 2$ and $\beta = 0.1$. The solid lines are the plot of $L^*_{c\geq 2} = L^*_{c\geq 2}(\alpha)$. The dashed lines are the critical value $\alpha = \alpha^*$.

The surprising result that the critical patch-size is not an increasing function of the speed with which the patch moves arises here as well. The curves for different values of $c$ intersect in both Figure 5.7 and Figure 5.8. To see the intersections more clearly in Figure 5.7, see Figure 5.9

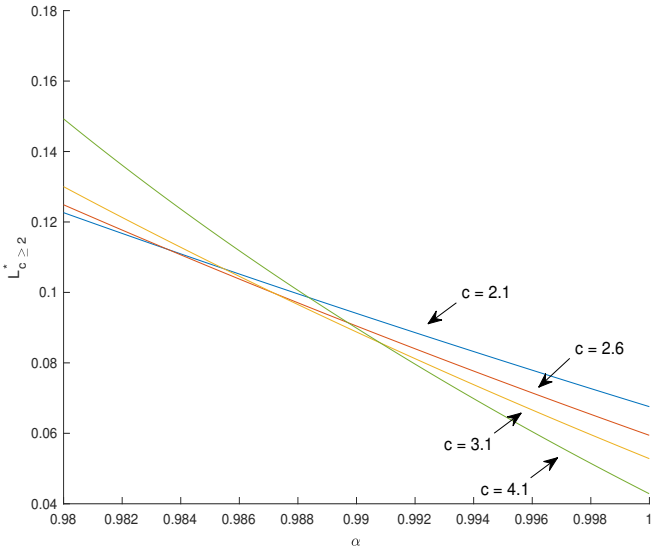


Figure 5.9: A close up of $L^*_{c\geq 2}$ as a function of the parameter $\alpha$ of the intersection of the plots. Model parameters are set to be $m_1 = m_2 = 1.4$, $D_1 = 1.1$, $D_2 = 2$ and $\beta = 0.9$.

As $\alpha$ decreases to the critical value $\alpha^*$ (indicated by the dashed line), the critical patch-size increases to infinity. The threshold $\alpha^*$ is an increasing function of $c$. Thus, as the speed of climate change increases, it becomes increasingly important for individuals to detect the trailing edge of the suitable habitat and to adjust their movement behaviour. If the patch is moving fast, individuals that leave the patch at the trailing edge have only a very small chance to ever catch up again. Hence, persistence is possible only if individuals do not leave the patch in the first place.

As before, I note that $L^*_{c\geq 2}$ is more sensitive to changes in $\alpha$ as $c$ is larger and less so when $\alpha$ is larger.

In this chapter, I illustrated how the critical patch-size depends on model parameters. I observed that the preference for the suitable habitat at the trailing edge can substantially reduce the critical patch-size, even when the preference for the suitable habitat at the leading edge is low. I can explain this observation by the direction in which the suitable patch moves. When individuals are leaving at the leading edge they can eventually be picked back up into their favoured habitat; when they leave at the trailing edge, it is unlikely that they reach the suitable habitat again.

# Chapter 6

# Discussion

## 6.1 Mathematical Results

As global temperatures continue to rise, mathematical analysis of range-shift models becomes increasingly important. The landmark papers published by Potapov and Lewis [10] and Berestycki et al. [3] provide a basis for this analysis. Both papers analyze a reaction-diffusion system on a domain represented by the real line. Defined on the real line is a bounded domain moving in one direction. Inside the domain growth occurs; outside, there is only mortality. The models in both papers are essentially the same; however, their approaches are different. Potapov and Lewis approach the problem by analyzing a system of two species with Lotka–Volterra competition dynamics. They use analytical methods mixed with numerical simulations to interpret the effect that the speed of the shifting interfaces has on the stability of the zero steady state. Berestycki et al. approach the problem from a geometrical analysis perspective with phase planes and consider only a single species. They also analyze the effect of the speed of the shifting interfaces with numerical simulations. In both papers, it is stated that there exists a critical speed $c^*$, beyond which a critical patch-size cannot be found and the zero steady state is always stable.

My thesis centres around the analysis of a single species living in such a range-shifting habitat. I, too, use the same idealized domain. I added to this analysis by incorporating the generalized boundary conditions derived by Maciel and Lutscher [9]. I use analytical techniques as well as phase planes to understand the effect of the moving interfaces on the stability of the zero steady state.

My results show that incorporating movement behaviour at the edges of a moving domain significantly changes the conditions under which a population can persist. Particularly, as the left-hand boundary approaches a Neumann-type condition, a critical domain size can be found for speeds faster than the asymptotic rate of spread on a homogeneous domain. In my model, this speed is given by $c^* = 2$. This is a new result that comes strictly from considering this movement behaviour.

It was shown in Chapter 5 that, for $c < c^*$, a small preference for the suitable habitat at the trailing edge requires a large domain size to sustain the population. It was shown in the illustrations that, as the preference was increased, the critical domain-size decreased.

A surprising observation was made that, regardless of the leading-edge behaviour, if the preference for the suitable habitat at the trailing edge is high enough, then a faster moving domain gives way to a smaller critical domain-size. In other words, $L^*$ is not monotone increasing in $c$ (for fixed $\alpha$ close to unity). The interpretation is that, as the speed of the edges increases, the individuals at the leading edge continue to be swept back into the domain. This happens at a faster rate for larger values of $c$.

This observation makes clear the importance of individual behaviour at the trailing edge. The conclusion is that if individuals can track the trailing edge and have a strong bias towards the suitable habitat, then the ability of the population to persist is greatly increased.

Another observation was the different impact that diffusion rates outside the bounded domain have on the critical patch-size. I observed that high diffusion rates behind the trailing edge correspond to smaller critical patch-sizes, but the opposite correlation is observed for diffusion rates in front of the leading edge. This suggests that high diffusion rates at the trailing edge may correspond to a better ability to track the shifting habitat, but high diffusion rates in front correspond to individuals "running away" from their suitable habitat.

## 6.2 Future Work

This thesis is, in a way, a generalization of papers [3] and [10]. However, Berestycki et al. [3] include an analysis on the population profiles. They found that, as $c$ increased, the population profile showed heavy asymmetry. The profile in front of the leading edge became steeper, and the profile behind the trailing edge became more gradual. The authors state that a steeper profile is easier to track than a gradual one, and thus tracking range shifts is easier to do at the leading edge. Their simulations, however, were restricted to the case of continuous density across the boundaries and consequently to a habitat moving at a speed slower than $c^*$. I suspect that if this analysis is done with the generalized boundary conditions as in my model, the population profile may take completely different shapes for different edge behaviour. I presume that, in the case of a strong bias at the trailing edge and weak bias at the leading edge, the population profile may take an opposite asymmetry, with a steep profile at the back and a gradual profile at the front. If at both edges there is a strong bias, I would expect to see less asymmetry. As well, the slope of the population profile for a discontinuity at an edge could change rather abruptly. The slope of the population profile could be studied as a function of the new model parameters $\alpha$ and $\beta$ as well

as the diffusion rates and speed of the interfaces. As well, population profiles need to be studied for habitats that are moving at a speed faster than $c^*$ as they did not arise in the previous works. This requires looking at the nonlinear model and would need numerical simulations.

Berestycki et al. [3] also looked at the extent of the range of the population and the total population size for different speeds $c < c^*$. They found that the extent grew with increasing $c$ but then quickly collapsed for $c$ close to $c^*$. I suspect that the same would be true in my model for a fixed bias at the trailing edge. Of course, if the right conditions are met, the extent could be positive for values of $c$ larger than $c^*$, but as the speed increases and the preference remains fixed, condition (4.3.17) would eventually no longer hold, and the extent would go to zero. This could likely correspond to an abrupt collapse of the population.

Another future project would be to perform this analysis for two competing species as done by Potapov and Lewis [10]. The authors studied the conditions under which two competing species could persist in a moving habitat. The authors applied Lotka–Volterra competition dynamics. The Lotka–Volterra model has been well studied, and the conditions for coexistence or competitive exclusion are well known. These outcomes can be predicted by comparing the growth rate and interspecies competition coefficients. The authors transformed the speed of the moving habitat into the growth function and found what they termed 'speed-induced mode switching'. What this means is that, with increasing $c$, their new growth function induced different dynamics in the model, so that the asymptotic outcome switched from one to another. They showed that, as $c$ increased, the competitive advantage shifts to the species with the larger $c^*$, even if the species with the smaller $c^*$ should win the competition. However, with my model, the threshold $c^*$ is not quite so strong a threshold as shown in Chapter 4. Thus, numerical simulations under the right assumptions may result in different mode switching, and a different outcome may occur. Potapov and Lewis [10] also found that, in the case where species one is established, then the outcome depends on where species two is introduced. If species two is introduced at the trailing edge, then, under suitable conditions for the speed of the invasion front, species two can successfully invade and species one becomes extinct. However, under the same conditions, if species two is introduced at the left boundary, it will quickly become extinct and species one wins. Again, this has not been analyzed for the case of generalized boundary conditions. It is clear that boundary behaviour plays a crucial role, so it is important to reassess these conclusions. What is clear to me is that the ability for the species to grow near the trailing edge is important. If the preference for the suitable habitat is low at the boundary, then the population is less likely to be able to grow fast enough there, which could be detrimental to its persistence.

In Section 2.4, I presented the derivation for the jump in density as done by Maciel and Lutscher [9]. Under different assumptions on parameter values, two different measures could be found. Characterizing these two different measures was the

fraction $\frac{D_1}{D_2}$. In one measure, it was without a square root; in the other, it included a square root. In my analysis, I considered only the former. It is not clear to me how the critical patch-size would change as a function of diffusive rates if the latter was considered instead. However, as this fraction appears in the denominator of the boundary conditions in the corresponding bounded problem, it would be a good project to compare the different effects on the critical patch-size for the different measures of the jump in density.

The presence of an Allee effect in moving habitat models has recently begun to be studied. An Allee effect arises if the highest per capita growth rate occurs not at $u = 0$ but at some intermediate point $u_b > 0$. Roques et al. [11] numerically analyzed the persistence of a species in a moving-habitat model with and without Allee effect. Generalized boundary conditions could be added to this numerical study.

In conclusion, the boundary behaviour at the trailing edge plays a critical role for species persistence in a moving habitat. In contrast to previous studies, conditions were found that allowed persistence of the species in its local habitat even for $c > c^*$. For fixed $c > c^*$, this condition is obtained for specific movement behaviour at the trailing edge.

# Appendix A

# Derivation of the Heat Equation via a Random Walk

The diffusion equation as a model for movement of individuals may be derived from a random walk approach [13]. I present the derivation on a one-dimensional lattice with intervals of length $\delta$. In each time step of length $\tau$, an individual moves one lattice point to the right or left with probability $p/2$. I denote by $P(x,t)\delta$ the probability that an individual is located in an interval of length $\delta$ centered at location $x$. The following master equation for $P$ is obtained from keeping track of where an individual moves:

$$P(x,t+\tau) = \frac{p}{2}P(x-\delta,t) + \frac{p}{2}P(x+\delta,t) + (1-p)P(x,t). \tag{A.1}$$

As $\tau$ and $\delta$ are assumed small, a natural first step is to expand Taylor series. This results, after the rearrangement of terms, in the equation

$$P_t(x,t) = \frac{p\delta^2}{2\tau}P_{xx}(x,t) + \mathcal{O}(\tau,\delta^3). \tag{A.2}$$

One now takes the so-called parabolic limit where $\delta, \tau \to 0$ in such a way that $\lim_{\delta,\tau\to 0} \frac{p\delta^2}{2\tau} = D$ is positive and finite. Thus, in the parabolic limit, equation (A.2) becomes the diffusion equation

$$P_t(x,t) = DP_{xx}(x,t). \tag{A.3}$$

# Bibliography


[1] IPCC (2007). *Climate Change 2007: Synthesis Report. Contribution of working groups I, II and III to the fourth assessment report of the intergovernmental panel on climate change.* Core Writing Team and R. K. Pachauri and A. Reisinger and IPCC, Geneva.

[2] D. Aronson and H. Weinberger. Nonlinear diffusion in population genetics, combustion, and nerve pulse propagation,. In *Partial Differential Equations and Related Topics*, number 446, pages 5 – 49. Springer, 1975.

[3] H. Berestycki, O. Diekmann, C.J. Nagelkerke, and P.A. Zegeling. Can a species keep pace with a shifting climate? *Bulletin of Mathematical Biology*, 71:339–429, 2009.

[4] R.S. Cantrell and C. Cosner. *Spatial Ecology via Reaction Diffusion Equations.* John Wiley and Sons, Ltd, Chichester, U.K., 2004.

[5] M. A. Harsch, Y. Zhou, J. HilleRisLambers, and M. Kot. Keeping pace with climate change: Stage-structured moving-habitat models. *The American Naturalist*, 184(1):25–37, July 2014.

[6] H. Kierstead and L. B. Slobodkin. The size of water masses containing plankton blooms. *Journal of Marine Research*, 12:141–147, 1953.

[7] S. J. Leroux, M. Larrivèe, V. Boucher-Lalonde, A. Huford, J. Zuloaga, J. T. Kerr, and F. Lutscher. Mechanistic models for the spatial spread of species under climate change. *Ecological Applications*, 23(4):815–828, 2013.

[8] D. Ludwig, D.G. Aronson, and H.F. Weinberger. Spatial patterning of the spruce budworm. *Journal of Mathematical Biology*, 8:217–258, 1979.

[9] G. A. Maciel and F. Lutscher. How individual movement response to habitat edges affects population persistence and spatial spread. *The American Naturalist*, 182(1):42–52, July 2013.

[10] A. B. Potapov and M. A. Lewis. Climate and competition: The effect of moving range boundaries on habitat invasibility. *Bulletin of Mathematical Biology*, 66:975–1008, 2004.

[11] R. L. Roques, H. Berestycki, and A. Kretzschmar. A population facing climate change: join influences of allee effects and evironmental boundary geometry. *Population Ecology*, 50:215–225, 2008.

[12] J. G. Skellam. Random dispersal in theoretical populations. *Biometrika*, 38:196–218, June 1951.

[13] P. Turchin. *Quantitative Analysis of Movement: measuring and modeling population redistribution of plants and animals*. Sinauer Assoc., 1998.

[14] G.-R. Walther, E. Post, P. Convey, A. Menzel, C. Parmesan, T. J. C. Beebee, J. M. Fromentin, O. Hoegh-Guldberg, and F. Bairlein. Ecological responses to recent climate change. *Nature*, 416:389–395, 2002.

[15] Y. Zhou and M. Kot. Discrete-time growth-dispersal models with shifting species ranges. *Theoretical Ecology*, 4:13–25, 2011.